A TWO-LAYER MOISTURE PREDICTION MODEL

by

JAMES AUGUSTINE ROBERT NEILON
A. B., Saint Anselm's College
(1953)

and

ROBERT BYRON WASSALL
B. S., The Pennsylvania State College
(1952)

SUBMITTED IN PARTIAL FULFILLMENT
OF THE REQUIREMENTS FOR THE
DEGREE OF MASTER OF
SCIENCE
at the
MASSACHUSETTS INSTITUTE OF
TECHNOLOGY
June 1965

Signature of Authors.....

Department of Meteorology, May 21, 1965

Certified by.....
Thesis Supervisor

Accepted by .....
Chairman, Departmental
Committee on Graduate Students

A TWO-LAYER MOISTURE PREDICTION MODEL

by

James Augustine Robert Neilon

and

Robert Byron Wassall

Submitted to the Department of Meteorology
on May 21, 1965 in partial fulfillment of the requirement
for the Degree of Master of Science

ABSTRACT

A two-layer moisture prediction model using vertically-integrated moisture fields is developed. The predicted fields of the moisture parameter, virtual precipitable water, are determined in the 1000-mb to 700-mb and 700-mb to 500-mb layers by horizontal advection by an appropriate steering wind and by the effect of vertical motion at the ground and at 650-mb. The vertical motion terms contain the contributions of horizontal divergence and vertical transport. It is shown that the contribution due to divergence is the more important of these in the lower layer while that due to vertical transport is of greater consequence in the upper layer. From the forecast of virtual precipitable water in each layer the mean relative humidity and precipitation amount is determined. Several experimental forecasts are examined and the feasibility of such a formulation is concluded on the basis of the realistic horizontal and vertical moisture patterns predicted by the model.

Thesis Supervisor: Frederick Sanders

Title: Associate Professor of Meteorology

ACKNOWLEDGEMENT

The authors wish to express their gratitude to Professor Frederick Sanders for suggesting this study and for providing valuable guidance during its completion.

We also thank Miss Isabel Kole for drafting the figures, Donald Rosenfeld for computational assistance and Peter Ottman of the National Meteorological Center for supplying data.

TABLE OF CONTENTS

I. INTRODUCTION

The recent success of a vertically integrated moisture model for the objective prediction of clouds and precipitation (Younkin, LaRue, and Sanders, 1965) has demonstrated the feasibility of the integrated approach in contradistinction to that of treating moisture content at separate levels (Smagorinsky and Collins, 1955, and Carlstead, 1959). A fundamental restriction of this method, however, is the inability to infer the vertical distribution of the predicted elements. The purpose of this investigation is to develop and test a two-layer vertically integrated moisture model. The derivation follows closely the work of Sanders who formulated a model for the prediction of the mass of water vapor in a single layer from 1000-mb to 500-mb.[1]

The desirability of a two-layer model stems from two distinct sources. The one is the more obvious, the quest for a modicum of resolution in the vertical. The other is the more pertinent, the observed distribution of condensation and water vapor transport. In an early work on quantitative precipitation forecasting the Staff Members, Tokyo University (1955), showed that the vertical cross section of condensation distribution along 90°W revealed two distinct centers: in the southern part the maximum of condensation was found in the layer between 1000-mb and 700-mb, while near 50°N condensation occurred mainly between 700-mb and 500-mb.

Benton and Estoque (1954), in a study of the water vapor transport

---

[1]Sanders, F., 1963: A Prediction Model for Integrated Water Vapor, Cloudiness and Precipitation, in Final Report Contract No. AF19(604)-8373, Dept. of Meteorology, MIT.

over and in the vicinity of the North American continent for the year 1949, found that the annual moisture flux over the area is accomplished by two well-defined streams, the one a strong southerly flow from the Gulf of Mexico and the other a weaker westerly current from the Pacific Ocean. The two merge over the central portion of the United States, resulting in a strong, broad outflow over the East Coast. These two streams are of essentially different character. Near the source region the southerly current has its maximum intensity in the low layer with 75% of the inflow occurring below 700-mb. But in the outflowing stream over the East Coast, 40% of the moisture occurs above 700-mb, probably reflecting the convective, frontal, and orographic lifting over the United States.

These researches seem to indicate that two layers are sufficient to represent the more important features of the observed moisture distribution and it was a logical choice to select the 1000-mb to 700-mb layer as the lower one and the 700-mb to 500-mb layer as the upper one. Although it is generally accepted that the low moisture content above 500-mb may be safely disregarded, a division into a 1000-mb to 650-mb and 650-mb to 400-mb layer was seriously considered. The chief advantage to this partition is that the currently available dynamically computed vertical motion field applies at 650-mb. No assumption concerning the vertical velocity profile would be necessary to obtain this field at the interface where it is of perhaps the greatest importance. This would not remove the need for a model of the profile, however, since the divergence distribution

is related to it. Disadvantageously, extension to 400-mb would render more difficult any comparison with present models which terminate at 500-mb. Finally, computed values of moisture parameters in the layers from 1000-mb to 700-mb and 700-mb to 500-mb were available from the National Meteorological Center.

With these considerations as background a two-layer model for the prediction of the mass of water vapor from 1000-mb to 500-mb was formulated. Mean relative humidity in the two layers and areas of precipitation may be inferred. The testing of the model comprised three twelve-hour forecasts made by manual Lagrangian technique. The evaluation was based on comparison with a forecast made by the model already alluded to (Younkin, LaRue, and Sanders, 1965) and on verification by actual observations.

II. FORMULATION OF THE PREDICTION MODEL

This model is derived in terms of a vertically integrated moisture parameter, precipitable water. Since we wish to make use of two layers we define the precipitable water for a layer as follows:

$$W \equiv \frac{1}{g} \int_{p_1}^{p_2} q \, dp \qquad (1)$$

where W is the mass (or liquid depth) of water vapor in a column of unit cross sectional area extending between the two pressure levels p_1 and p_2, g is the acceleration of gravity, and q is the specific humidity.

With the assumption of no evaporation or condensation the total mass of water vapor in the atmosphere is a conservative quantity. As suggested by the Staff Members of Tokyo University (1955) we designate this quantity the virtual precipitable water, W'. Similarly, q', the virtual specific humidity, is conserved. Therefore, local changes are due to the three-dimensional divergence of the specific humidity transport vector. This may be expressed

$$\frac{dq'}{dt} = 0 \tag{2}$$

$$\frac{\partial q'}{\partial t} = -\nabla \cdot q\vec{V} - \frac{\partial q\omega}{\partial p} \tag{3}$$

$$= -\vec{V} \cdot \nabla q - q\nabla \cdot \vec{V} - \frac{\partial q\omega}{\partial p} \tag{4}$$

where $\vec{V}$ is the horizontal wind vector, $\omega \equiv dp/dt$, the vertical velocity in the x, y, p, t co-ordinate system which is used throughout this formulation.

Partial differentiation of the "virtual" form of (1) followed by integration of (4) between constant pressure levels p_1 and p_2 gives the local rate of change of the virtual precipitable water.

$$\frac{\partial W'}{\partial t} = \frac{1}{g}\int_{p_1}^{p_2}(-\vec{V} \cdot \nabla q)\,dp + \frac{1}{g}\int_{p_1}^{p_2}(-q\nabla \cdot \vec{V})\,dp + \frac{1}{g}\left[(q\omega)_{p_2} - (q\omega)_{p_1}\right] \tag{5}$$

The local rates of change of the virtual precipitable water in the lower and upper layers are given by

$$\frac{\partial W_e'}{\partial t} = \frac{1}{g}\int_{700}^{1000}(-\vec{V}\cdot\nabla q)\,dp - \frac{1}{g}\int_{700}^{1000}(-q\,\nabla\cdot\vec{V})\,dp + \frac{1}{g}\left[(q\omega)_{700} - (q\omega)_{1000}\right] \quad (6)$$

$$\frac{\partial W_u'}{\partial t} = \frac{1}{g}\int_{500}^{700}(-\vec{V}\cdot\nabla q)\,dp + \frac{1}{g}\int_{500}^{700}(-q\,\nabla\cdot\vec{V})\,dp + \frac{1}{g}\left[(q\omega)_{500} - (q\omega)_{700}\right] \quad (7)$$

From this formulation it is apparent that the local changes of virtual precipitable water in a layer are due to causes identified with the three terms on the right hand side of equation (5), namely, the integrated effect of the horizontal advection of moisture, the integrated effect of the horizontal divergence of the wind on the moisture, and the net effect of the moisture transport across the upper and lower boundaries of the layer.

We now attempt to obtain suitable expressions for these integrals in terms of parameters which are readily available. This involves modeling the vertical profiles of specific humidity, horizontal winds and divergence of the wind. The success of this prediction method is commensurate with the accuracy of such models. We assume the same form of the profiles as did Sanders in a previously cited report.

To evaluate moisture advection we require profiles for the vertical variation of specific humidity and of the wind within each layer. We shall assume that

$$q_e(p) = \frac{\alpha_e(p)\,W_e\,g}{300\,mb} \quad (8)$$

and

$$q_u(p) = \frac{\alpha_u(p)\,W_u\,g}{200\,mb} \quad (9)$$

where α_ℓ and α_u are modeling parameters.

Profiles of α were computed from specific humidity data averaged for a group of ten upper air stations in continental United States. The stations, selected to include a representative sampling of climatic and topographic regimes, consisted of Caribou (712), Columbia, Mo., (445), Denver (469), International Falls (747), Lake Charles (240), Oakland (493), Pittsburgh (520), Spokane (785), Tampa (211), and Tucson (274). One-hundred and twenty individual soundings from the months of January, April, July, and October for the years 1961 to 1963 were chosen at random and averaged to obtain the desired specific humidity data. Where humidity data were missing, a relative humidity of 20% was assumed. The Denver profile was extrapolated from the surface to 1000-mb so as to parallel the mean profiles of the other stations. Published mean monthly sounding readily available in Climatological Data were not used because of the frequent absence of humidity data for the 500-mb level.

Profiles were prepared for each of the four months in an attempt to detect any significant seasonal differences that might exist. The resultant profiles showed marked similarity in the 700-mb to 500-mb layer and only minor deviations in the 1000-mb to 700-mb layer where the July profile indicated a slightly slower decrease of moisture with altitude than in the other months. Considering the limitations imposed by the sample size and the lack of any apparent noteworthy deviation in seasonal profiles, overall average profiles (Fig. 1) were computed and used in the developement of the prediction equations.

For the horizontal wind vector a simple profile for each layer is assumed in which the wind at any pressure level within the layer is expressed as the vector sum of the wind at the base of the layer and a constant times the wind shear vector between the bottom and the top of the layer.

$$\vec{V}_\ell(p) = \vec{V}_{1000} + \beta_\ell(p)(\vec{V}_{700} - V_{1000}) \tag{10}$$

$$\vec{V}_u(p) = \vec{V}_{700} + \beta_u(p)(\vec{V}_{500} - \vec{V}_{700}) \tag{11}$$

where β_ℓ and β_u are modeling parameters.

Profiles of β were computed from monthly mean soundings published in Climatological Data for the years 1961 to 1963. Data were compiled from the same moths and for the same stations as considered for the α profiles. The procedured used were the same as Sanders (1963).[1]

As in the case of the α profiles, the upper layer profiles showed a marked seasonal similarity. There were greater variations between the lower level profiles, however, where July in particular stood apart from the others. In contrast to a nearly linear increase of wind speed with altitude in the other months, the July profile suggested that winds in the lower portion of the 1000-mb to 700-mb layer were on the average almost as strong as those at 700-mb. There was also a tendency for a slight decrease in speed between 900-mb and 850-mb. This characteristic was most apparent at the southern stations where the overall wind flow was rather light. The October profile showed some tendency towards the same type of distortion

[1] op. cit.

from a linear increase but not nearly to the magnitude of the July profile. The observed variations were comparable to those noted by Headlee (1965)[1] in his study on effective moisture steering levels.

An overall average profile (Fig. 1) was used for both levels in this study but it appears that a separate low level profile would probably be more appropriate for the summer season at least.

Making use of these derived relationships for specific humidity and the horizontal wind vector the integrated effect of moisture advection in (6) and (7) may be written

$$\frac{1}{g}\int_{700}^{1000}(-\vec{V}\cdot\nabla q)\,dp = -\vec{V}_l^{*}\cdot\nabla W_l \qquad (12)$$

and

$$\frac{1}{g}\int_{700}^{500}(-\vec{V}\cdot\nabla q)\,dp = \vec{V}_u^{*}\cdot\nabla W_u \qquad (13)$$

where

$$\vec{V}_l^{*} = K_1\vec{V}_{1000} + K_2\vec{V}_{700}$$

$$\vec{V}_u^{*} = K_3\vec{V}_{700} + K_4\vec{V}_{500}$$

$$K_1 \equiv \frac{1}{300\text{mb}}\int_{700}^{1000}\alpha_l(1-\beta_l)\,dp = .57$$

$$K_2 \equiv \frac{1}{300\text{mb}}\int_{700}^{1000}\alpha_l\beta_l\,dp = 1-K_1 = .43$$

$$K_3 \equiv \frac{1}{200\text{mb}}\int_{500}^{700}\alpha_u(1-\beta_u)\,dp = .58$$

$$K_4 \equiv \frac{1}{200\text{mb}}\int_{500}^{700}\alpha_u\beta_u\,dp = 1-K_3 = .42$$

[1] Headlee, H. E., 1965: A Study of the Effective Moisture-Steering Level in a Cloud and Precipitation Prediction Model, M. S. Thesis, Dept. of Meteorology, M. I. T.

Computed values of K_1 and K_3 for the ten stations used in the evaluation are shown in Table 1. At the low latitude stations a rather light wind pattern characterized by a decrease in speed with altitude existed at times during the Julys under study causing rather erratic values of K_1 for that month. Headlee experienced similar difficulty by arriving at a K_1 value of -5.77 for Lake Charles in July 1961. The modeling approximation for wind speed loses significance on occasions when the wind speed near the lower boundary of the layer is nearly equal to that at the upper boundary. Thus, when evaluating $\mathcal{B}$ for a layer, soundings with a small vertical wind shear should be omitted.

To evaluate the contribution of the effect of divergence we require profiles for the vertical variation of divergence together with that of the specific humidity. It is desirable to express the divergence in terms of vertical velocity at the bottom boundary and at 650-mb since that is regularly available. Because the vertical velocity at only one intermediate level in the layer from 1000-mb to 500-mb was available, nothing could be gained by modeling the divergence in the two layers independently and the assumed profile of divergence is as follows:

$$\nabla\cdot\vec{V}(p) = -\frac{\omega_{1000}}{1000\,mb} + B(p)\left(\nabla\cdot\vec{V}_{650} - \nabla\vec{V}_{1000}\right) \qquad (14)$$

The profile of B was derived from Buch's data averaged for mid-latitudes.[1] It is essentially a linear function of pressure between 1000-mb and 500-mb.

[1]Buch, H. S., 1954: Hemispheric Wind Conditions During the Year 1950, M. I. T., Dept. of Meteorology, Final Report, General Circulation Project.

From the integrated equation for the continuity of mass

$$\omega(p) = \int_p^0 \nabla \cdot \vec{V}\, dp \tag{15}$$

The expression for ω at 650-mb is

$$\omega_{650} = \int_{650}^0 \nabla \cdot \vec{V}\, dp \tag{16}$$

Integrating (14) between 650-mb and the top of the atmosphere

$$\omega_{650} = \int_{650}^0 \nabla \cdot \vec{V}\, dp = 0.65\,\omega_{1000} - C_{650}\left(\nabla \cdot \vec{V}_{650} - \nabla \cdot \vec{V}_{1000}\right) \tag{17}$$

where $C_{650} \equiv \int_0^{650} B\, dp$

The divergence at any level p may be expressed also in terms of and ω_{650}. Solving (17) for the coefficient of C_{650}

$$\left(\nabla \cdot \vec{V}_{650} - \nabla \cdot \vec{V}_{1000}\right) = \frac{.65\,\omega_{1000} - \omega_{650}}{C_{650}} \tag{18}$$

and substituting in (14) yields

$$\nabla \cdot \vec{V}(p) = \frac{-\omega_{1000}}{1000\ mb} + B(p)\left(\frac{.65\,\omega_{1000} - \omega_{650}}{C_{650}}\right) \tag{19}$$

$$= \left(\frac{.65\,B(p)}{C_{650}} - 10^{-3}\ mb^{-1}\right)\omega_{1000} - \frac{B(p)}{C_{650}}\,\omega_{650} \tag{20}$$

Making use of this relationship the divergence terms in (6) and (7) may be written

$$\frac{1}{g}\int_{500}^{700} -q\, \nabla \cdot \vec{V}\, dp = K_5 W_e\, \omega_{1000} + K_6 W_e\, \omega_{650} \tag{21}$$

and

$$\frac{1}{g}\int_{500}^{700} -g\nabla\cdot\vec{V}\,dp = K_7 W_u \omega_{1000} + K_8 W_u \omega_{650} \qquad (22)$$

where $$K_5 \equiv \frac{10^{-3} mb^{-1}}{300 mb}\int_{700}^{1000}\alpha_e(p)\,dp - \frac{0.65}{(300mb)(C_{650})}\int_{700}^{1000}\alpha_e(p)\,B(p)\,dp$$

$$K_6 \equiv \frac{1}{(300mb)(C_{650})}\int_{700}^{1000}\alpha_e(p)\,B(p)\,dp$$

$$K_7 \equiv 5\times10^{-6} mb^{-2}\int_{500}^{700}\alpha_u\,dp - \frac{3.25\times10^{-3} mb^{-1}}{C_{650}}\int_{500}^{700}\alpha_u B\,dp$$

$$K_8 \equiv \frac{5\times10^{-3} mb^{-1}}{C_{650}}\int_{500}^{700}\alpha_u B\,dp$$

From the profiles of the modeling parameters (Fig. 1) the terms in the definition of these constants are evaluated.

C_{650} = 203 mb

$\int_{700}^{1000}\alpha_e\,dp$ = 153 mb

$\int_{700}^{1000}\alpha_e B_e\,dp$ = -32.25 mb

$\int_{500}^{700}\alpha_u\,dp$ = 101 mb

$\int_{500}^{700}\alpha_u B_u\,dp$ = -14.25 mb

The constants themselves are now given by

$K_5 = 8.54 \times 10^{-4} mb^{-1}$

$K_6 = -5.29 \times 10^{-3} mb^{-1}$

$K_7 = 7.33 \times 10^{-4} mb^{-1}$

$K_8 = -3.51 \times 10^{-4} mb^{-1}$

The vertical transport term may be evaluated by deriving suitable expressions for ω_{700} and ω_{500}. Using (15) and integrating (14)

$$\omega(p) = \left(p \times 10^{-3} - \frac{.65 C(p)}{C_{650}}\right)\omega_{1000} + \frac{C(p)}{C_{650}}\omega_{650} \qquad (23)$$

Therefore,

$$\omega_{700} = \left(.70 - \frac{.65 C_{700}}{C_{650}}\right)\omega_{1000} + \frac{C_{700}}{C_{650}}\omega_{650} \qquad (24)$$

and

$$\omega_{500} = \left(.50 - \frac{.65 C_{500}}{C_{650}}\right)\omega_{1000} + \frac{C_{500}}{C_{650}}\omega_{650} \qquad (25)$$

Now that we are in a position to evaluate the vertical transport term it is pertinent to examine it in more detail. As has been pointed out this represents the resultant of the moisture transport across the upper and lower boundaries of a column which extends between two fixed pressure levels. Realistically there is no flux of mass through the bottom boundary in the lower levels since it represents the ground level (or below) except where the surface pressure is greater than 1000-mb. The fact that the lower layer does not everywhere extend to 1000-mb cannot be ignored even though this does violence to our previous modeling assumptions. Sanders (1963)[1] discusses this problem of orographic effects in some detail and concludes, on the basis of analysis of the character and consistency of the

[1] op. cit.

of the errors made in the forecasts in the vicinity of the Rockies, that the internal inconsistency of considering a variable pressure at the bottom boundary is preferable to the error involved in being consistent but unrealistic. In view of this evidence the vertical transport across the bottom boundary of the lower layer is set to zero.

As a result the vertical transport term in (6) for the layer from 1000-mb to 700-mb may be expressed in terms only of the flux across the top boundary. Utilizing the relations expressed in (8) and (19)

$$\frac{1}{g}(qw)_{700} = \frac{1}{g}\left(\frac{\alpha_{700} W_e q}{300\,mb}\right)\left[(.70-.65\frac{C_{700}}{C_{650}})\omega_{1000}+\frac{C_{700}}{C_{650}}\omega_{650}\right] \qquad (26)$$

From the profiles of the modeling parameters $(\alpha_e)_{700} = .55$ and $C_{700} = 194$ mb.

$$\frac{1}{g}\left[(qw)_{700}-(qw)_{1000}\right] = K_9 W_e \omega_{1000} + K_{10} W_e \omega_{650} \qquad (27)$$

where $K_9 \equiv \frac{(\alpha_e)_{700}}{300mb}\left(.70-.65\frac{C_{700}}{C_{650}}\right) = 1.40\times10^{-4}\,mb^{-1}$

$$K_{10} \equiv \frac{(\alpha_e)_{700}}{300\,mb}\left(\frac{C_{700}}{C_{650}}\right) = 1.69\times10^{-3}\,mb^{-1}$$

The vertical transport term for the upper layer from (7) is evaluated in a straightforward manner using (9), (24), and (25).

$$\frac{1}{g}\left[(qw)_{500}-(qw)_{700}\right] = \frac{1}{g}\left[\left(\frac{(\alpha_w)_{500} W_w q}{200\,mb}\right)\left[(.50-.65\frac{C_{500}}{C_{650}})\omega_{1000}+\frac{C_{500}}{C_{650}}\omega_{650}\right]\right] - \frac{1}{g}\left[\left(\frac{(\alpha_w)_{700} W_w q}{200\,mb}\right)\left[(.70-.65\frac{C_{700}}{C_{650}}\omega_{1000}+\frac{C_{700}}{C_{650}}\omega_{650}\right]\right] \qquad (28)$$

With $(\alpha_w)_{700} = 1.57$, $(\alpha_w)_{500} = .45$, and $C_{500} = 197$ mb, this may be written

$$-\frac{1}{g}\left[(q\omega)_{500}-(q\omega)_{700}\right]=K_{11}W_{ue}\omega_{1000}+K_{12}W_{ue}\omega_{650}-K_{13}W_{ue}\omega_{1000}-K_{14}W_{ue}\omega_{650} \quad (29)$$

where $K_{11} \equiv \frac{\alpha_{500}}{200mb}\left(.50-.65\frac{c_{500}}{c_{650}}\right) = -2.95 \times 10^{-4} mb^{-1}$

$$K_{12} \equiv \frac{\alpha_{500}}{200mb}\frac{c_{500}}{c_{650}} = 2.18 \times 10^{-3} mb^{-1}$$

$$K_{13} \equiv \frac{(\alpha_{ue})_{700}}{200mb}\left(.70-.65\frac{c_{700}}{c_{650}}\right) = 6.20 \times 10^{-4} mb^{-1}$$

$$K_{14} \equiv \frac{(\alpha_{ue})_{700}}{200mb}\frac{c_{700}}{c_{500}} = 7.50 \times 10^{-3} mb^{-1}$$

A further examination of the vertical transport terms for both layers reveals that each contains the factor $(q\omega)_{700}$, since 700-mb is the top boundary for the bottom layer and the lower boundary for the upper layer. In the expansion of this factor in terms of the modeling parameters for each layer the transport through the interface is given in two forms

$$(q\omega)_{700}=(K_9W_e\omega_{1000}+K_{10}W_e\omega_{650})=(K_{13}W_{ue}\omega_{1000}+K_{14}W_{ue}\omega_{650}) \quad (30)$$

Both representations of this term should be equivalent but due to the modeling approximations they may not be in practice. An examination was made of this term for the data used as a test of this model over the eastern United States (where it was assumed that ω_{1000} was negligible). The data were taken from 25 radiosonde stations for each of three observing times. The values of ω_{650} were taken from the dynamically computed vertical velocities

from NMC. In the 25 cases of descending motion, the average instantaneous transport through the interface was, in absolute value, 3.64×10^{-7} cm/sec for the lower layer and 3.79×10^{-7} cm/sec for the upper layer. The difference represents a transport of .002 cm in 12 hours if continued at this rate. In the 50 cases of ascending motion the average transport rates were 1.10×10^{-6} cm/sec and 1.15×10^{-6} cm/sec, the difference between which represents .006 cm in 12 hours. On the average, therefore, the difference is small compared with the magnitudes of the transport and the two representations of flux through the interface at 700-mb may be considered equivalent. It must be noted, however, that there were stations for which the two transports did not agree. The maximum difference of .15 cm and .14 cm per 12 hours occurred at Lake Charles and Shreveport, respectively, at 00Z January 9, 1965. In this area was precipitable water in the lower layer on the order of ten times that in the upper layer and with moderately strong upward motion of about .0015 mb sec^{-1} these relatively large differences in transport across the interface result.

The horizontal divergence (21), (22) and vertical transport (27), (29) terms are expressed in terms of W and ω and may be combined for each layer.

$$\frac{1}{g}\left[\int_{700}^{1000}(-q\nabla\cdot\vec{v})\,dp + (q\omega)_{700} - (q\omega)_{1000}\right] = K_{15} W_\ell \omega_{1000} + K_{16} W_\ell \omega_{650} \qquad (31)$$

$$\frac{1}{g}\left[\int_{500}^{700}(-q\nabla\cdot\vec{v})\,dp + (q\omega)_{500} - (q\omega)_{700}\right] = K_{17} W_u \omega_{1000} + K_{18} W_u \omega_{650} \qquad (32)$$

where $K_{15} \equiv K_5 + K_9 = 9.94 \times 10^{-4} mb^{-1}$

$K_{16} \equiv K_6 + K_{10} = -3.60 \times 10^{-3} mb^{-1}$

$K_{17} \equiv K_7 + K_{11} - K_{13} = -1.82 \times 10^{-4} mb^{-1}$

$K_{18} \equiv K_8 + K_{12} - K_{14} = -5.67 \times 10^{-3} mb^{-1}$

It is reassuring to note that these coefficients are in agreement with synoptic experience as to sign and relative magnitudes. K_{15}, the coefficient of $W_2 \omega_{1000}$ in (31), is positive, indicating that an air column forced to rise due to orographic effect loses moisture while that which descends gains moisture. K_{16}, the coefficient of $W_2 \omega_{650}$, is negative, implying that upward motion near the top of the lower layer results in enrichment of the moisture in this layer. The explicit vertical transport term which involves K_{10} makes a negative contribution but the effect of horizontal convergence below (K_6) accompanying the rising motion gives a larger positive contribution.

The evaluation of K_{17} is somewhat more tenuous. The contribution to the moisture of the upper layer resulting from upward vertical motion induced by orography at the base of the lower layer is positive. This term is apparently insignificant, however, since K_{17} is nearly an order of magnitude smaller than K_{15}. For this reason the term involving ω_{1000} for the upper layer will be neglected. K_{18}, the coefficient of $W_m \omega_{650}$ in (32) is negative, indicating that upward vertical motion near the base of the layer increases the moisture in the layer. This is due both to the contribution from horizontal convergence and, more importantly, from the vertical transport.

Combining the evaluated terms and incorporating the several assumptions, (6) and (7) now have the form

$$\frac{\partial W_e'}{\partial t} = -\vec{V}_e^* \cdot \nabla W_e + K_{15} W_e \omega_{1000} + K_{16} W_e \omega_{650} \tag{33}$$

$$\frac{\partial W_w'}{\partial t} = -\vec{V}_w^* \cdot \nabla W_w + K_{18} W_w \omega_{650} \tag{34}$$

To perform the integration in time it is convenient to replace W where it occurs on the right hand side of the equations with W'. As defined previously the precipitable water W is identical to the virtual precipitable water W' at initial time and differs only as evaporation or condensation occurs. Division of both sides of the equations by W' yields

$$\frac{\partial \ln W_e'}{\partial t} = -\vec{V}_e^* \cdot \nabla \ln W_e' + K_{15} \omega_{1000} + K_{16} \omega_{650} \tag{35}$$

$$\frac{\partial \ln W_w'}{\partial t} = -\vec{V}_w^* \cdot \nabla \ln W_w' + K_{18} \omega_{650} \tag{36}$$

These prediction equations may be regarded as quasi-conservative. In the test cases to be described in a subsequent section, these equations were integrated by manual Lagrangian techniques over 12-hour periods. The trajectories were terminated at a regular network of points the distance between which was 782 km at 60°N.

For any forecast interval Δt the integrated prediction equations are

$$(\ln W_e')_{fd} = (\ln W_e')_{iw} + (K_{15} \bar{\omega}_{1000} + K_{16} \bar{\omega}_{650}) \Delta t \tag{37}$$

$$(\ln W_w')_{fd} = (\ln W_w')_{iw} + (K_{17}\bar{\omega}_{650})\Delta t \qquad (38)$$

The subscript fd refers to the forecast downstream value at the end point of the trajectory and iu refers to the initial upstream value at the beginning point.

The remaining problem is that of evaluating the vertical velocities. Diagnoses and forecasts of vertical motion at 650-mb are currently available from NMC in a scaled form such that

$$\hat{\omega}_{650} \equiv -\omega_{650} \times 10^3$$

Following the air column, the average value of the vertical motion experienced by it may be given by

$$\bar{\omega}_{650} = \tfrac{1}{2}\left[(\omega_{650})_{iw} + (\omega_{650})_{fd}\right] = \left[(\hat{\omega}_{650})_{iw} + (\hat{\omega}_{650})_{fd}\right](5\times10^{-4})$$

As a measure of $\bar{\omega}_{1000}$, the pressure change experienced by the base of the column during the forecast interval was used. Thus

$$\bar{\omega}_{1000} = (p_{fd} - p_{iw})/\Delta t$$

The standard atmospheric value for terrain heights were used in the computation of the pressure change. The heights of the terrain were based on the data of Berkofsky and Bertoni (1955) averaged over 5^o latitude-longitude squares. The choice of suitable topography is a difficult one but this one appears to be justified since we have chosen to attempt to depict

only the large scale moisture patterns.

With the time interval Δt = 12 hours = 4.32×10^4 seconds, the final forms of the forecast equations become

$$(\ln W'_w)_{fd} = (\ln W'_w)_{ini} + .004(p_{fd} - p_{ini}) + .078[(\hat{\omega}_{650})_{ini} + (\hat{\omega}_{650})_{fd}] \quad (39)$$

$$(\ln W'_m)_{fd} = (\ln W'_m)_{ini} + .122[(\hat{\omega}_{650})_{ini} + (\hat{\omega}_{650})_{fd}] \quad (40)$$

III. ESTIMATION OF MEAN RELATIVE HUMIDITY AND PRECIPITATION FROM THE MODEL.

The model as derived applies only to the forecast of virtual precipitable water. Since this is a rather artificial quantity it is of utmost interest to inquire what parameters of more immediate importance may be inferred from it. The virtual precipitable water has been defined as that amount which would be obtained by the three-dimensional transport under the assumption that neither condensation nor evaporation takes place. This quantity obviously allows for supersaturated conditions. It is desirable, therefore, to define a new value, W_s, which represents the amount of precipitable water that an air column can hold without condensation occurring. Unfortunately, this quantity is not uniquely defined by the parameters involved in the model. The mean temperature of each layer as represented by the thickness is available and this value has been used to estimate W_s. This is the procedure used by Sanders (1963)[1] and the limitations of the method are discussed by him.

[1] op. cit.

To derive the approximate relationships between the thickness of a layer and W_s in that layer, mean temperature profiles for fall and winter were used. These were derived from data from the Northern Hemisphere for the year 1950.[1] From the average temperatures at 1000-mb, 850-mb, 700-mb, and 500-mb, the thickness values of the layers from 1000-mb to 700-mb and 700-mb to 500-mb were computed assuming varying amounts of moisture represented by 100%, 80%, 60%, 40%, and 20% mean relative humidity. The results of these calculations relating the thickness in each layer to the precipitable water in terms of mean relative humidity is given in Figure 2.

It is not uncommon to observe condensation and precipitation in a layer with a mean relative humidity less than 100%. Younkin, LaRue and Sanders (1965) used a value of 70% relative humidity in the column extending from 1000-mb to 500-mb to connote saturation, justifying this figure by the low bias in radiosonde measurements of relative humidity and by observational evidence. There are some indications that this figure is too low, however. Newer humidity elements which are being introduced should remove the bias at least partially and it has been noted that the use of the 70% figure at the National Meteorological Center seems to result in precipitation areas which are too large. In any event, this refers to a deep layer approximately 5500 meters in standard thickness, while the two-layer model represents thicknesses on the order of one-half this depth. From one point of view it seems logical to demand a higher mean relative humidity for condensation in a shallower

[1] Peixoto, J. P., 1960: Hemispheric Temperature Conditions During the Year 1950, M.I.T., Dept. of Meteorology Scientific Report No. 4, Planetary Circulation Project.

layer, since in the limiting case, saturation is required for condensation at a given layer. It also seems plausible that for the upper layer in winter a lower mean relative humidity would be appropriate since the reported relative humidity is defined with respect to a plane water surface and in many cases the state of the moisture in the layer is frozen. This definition results in a low bias of relative humidity in ice clouds, but the effect is difficult to assess since undoubtedly there are also clouds at below freezing temperatures which consist mainly of water. It was decided, therefore, to give more weight to the first argument and to consider a mean relative humidity of 90% to be sufficient for condensation in either layer. The value assigned to W_s is that which represents 90% relative humidity.

Given the virtual precipitable water W', the actual precipitable water W and relative humidity in the layer can be estimated provided that the thickness is also known. If W' is less than W_s, it is assumed that W' = W and the relative humidity is taken directly from the nomogram. If W' exceeds W_s, it is assumed that W = W_s and the relative humidity is 90%. The excess amount, W' - W_s, is assumed to condense and fall as precipitation. A quantitative precipitation forecast is therefore a by-product of the forecast.

This procedure must be modified for locations in mountainous regions, since the lower layer does not extend to 1000-mb. The forecast value of W' applies to an entire 300-mb layer. The procedure adopted was to adjust the value of the virtual precipitable water to account for the restricted depth of the layer and also for the reduced value of α in the layer. The adjusted

value (W") is

$$W'' = W' \left[\frac{300}{(\pi - 700)\bar{r}} \right] \qquad (41)$$

where W' and $\bar{r}$ refer to the restricted layer between π, the station pressure, and 700-mb.

If W" exceeds W_s, the excess amount W" - W_s is reduced by the factor in brackets in (41) to arrive at the amount of precipitation. The standard atmosphere value corresponding to the station elevation was used as station pressure for this purpose.

IV. TESTS OF THE PREDICTION MODEL

The purpose of the test cases was to determine the appropriateness and goodness of the model postulated. To this end we wished to avoid errors introduced by using predicted values of the horizontal and vertical velocity fields. Observed fields were therefore used to displace the moisture pattern. Diagnostic fields of vertical motions from the currently operational three-level forecast model[1] were used and observed thickness patterns were used to determine relative humidity and W_s. There is no guarantee, of course, that the diagnostic vertical motion and observed thickness fields are completely consistent, in that over the forecast period, the observed thickness may not be that which would have been produced by horizontal advection and diagnostic vertical motions which are used in the specific humidity advection. The effect

[1] Cressman, G. P., 1963: A Three-Level Model Suitable for Daily Numerical Forecasting, National Meteorological Center Technical Memorandum No. 22.

of this inconsistency in this model is slight in most cases, however, since the thickness is used only to infer the relative humidity; in the one-layer model of Younkin, LaRue, and Sanders (1965) the effect is more apparent as the results of a test case will show.

The moisture prediction model was tested on the synoptic pattern which occurred between 0000 GMT January 8, 1965 and 0000 GMT January 9, 1965. This particular situation was chosen because of the existence of two distinct precipitation areas at the beginning of the 24-hour period followed by the development of a third area in the latter half of the period. This afforded an opportunity to test the model on the detection of new precipitation areas as well as the movement and modification of existing areas.

The surface map for 0000 GMT January 8, 1965 (Fig. 3) consisted of a north to south oriented high pressure ridge across New England bordered on the west by a broad southwesterly flow extending from the Gulf of Mexico to the eastern Great Lakes region. A weak, complex low pressure system covered the region from the western Great Lakes to the central Rockies. A warm front extended from Alabama northward to the vicinity of Cincinnati, Ohio then westward into the low pressure complex. A band of light rain was occurring to the north of the warm front in the lower Great Lakes region. An outbreak of cold air was spreading into the northern plains behind a cold front which had moved as far southward as the northern border of Nebraska. Another frontal system extending from Wyoming to extreme southwestern Arizona marked the forward edge of an anticyclone centered off the northern coast of California.

Precipitation was occurring in the onshore flow in the Pacific northwest and there were also a few scattered areas of light showers or snow flurries in the Rockies and in the northern plains.

The associated 500-mb flow pattern consisted of full latitude troughs at about 60°W and at about 115°W with a tendency for a cut-off low in southwestern United States. A broad southwesterly flow existed from the Rockies to a ridge located just west of the Appalachian Mountains. In the 24-hour period which followed, a cut-off low did form over New Mexico while the higher latitude portion of the trough sheared and moved eastward to the Minnesota-Wisconsin region. Southwesterly flow continued from Texas to the ridge which had shifted to the Atlantic coast.

At the surface (Figs. 4 and 5) southwesterly flow overspread the entire east coast as the high pressure ridge moved offshore. The complex low pressure area consolidated into a single center and intensified while moving to a position just south of James Bay. The warm front moved to the Washington-Buffalo line while the primary cold front traveled eastward and southward to a line from the upper Great Lakes region across southeastern Missouri to northcentral Texas. In the far west the anticyclone moved inland with its center now located over Nevada. Precipitation at 0000 GMT January 9 consisted of a newly developed region extending from central Illinois to eastern Oklahoma as well as the previously existing areas in the northeast and in the Pacific northwest.

Twelve-hour forecasts valid at 1200 GMT January 8, 1965 and at 0000 GMT January 9, 1965 were prepared using the observed flow for both initial and

terminal conditions and using the observed precipitable water to describe initial moisture conditions. A third 12-hour forecast, this one also valid at 0000 GMT January 9, was prepared using precipitable water predicted in the earlier forecast as initial moisture rather than the observed quantities. This forecast is referred to as a 24-hour forecast in the discussion which follows. Forecasts of upper layer and lower layer moisture were made for each time with initial results expressed in terms of virtual precipitable water.

Determining the value of the advection term in the forecast equations required the greatest expenditure of effort in the forecast procedure. The first step called for the construction of the moisture steering flow at each of the map times and for both layers. The 1000-mb, 700-mb and 500-mb geopotential heights at an array of grid points were multiplied by the appropriate values of K_1, K_2, K_3, and K_4. The products were summed at each of the grid points to arrive at values of the moisture steering flow for the layer in question (Figs. 8, 9, 10, 11, 27, and 28).

Twelve-hour trajectories terminating at each of the grid points were constructed in the moisture steering flow. From each grid point trajectories were backed six hours upstream in the flow which existed at the termination of the trajectories and then another six hours in the flow which existed 12 hours earlier. Initial values of precipitable water were advected from these upstream points.

The other terms in the prediction equations were also evaluated using the trajectories in the moisture steering flow to arrive at initial upstream and

terminal downstream values of the quantities measured. Essential features of the vertical velocity fields at 650-mb are shown on the surface maps (Figs. 3, 4, and 5).

From the forecast values of virtual precipitable water, values of precipitable water, relative humidity, and precipitation amount were estimated using the procedure outlined in Section III. In those cases when W' exceeded W_s, the excess amount was considered as the precipitation amount at the termination point of the trajectory. While this approach may be unrealistic, no universally satisfactory manner of treating this problem is evident. It is clear that the procedure adopted has certain limitations. For example, the fact that W' exceeds W_s at the end point of the trajectory implies that W' equalled W_s at some point upstream and according to our convention precipitation should have begun there. However, it is difficult to ascertain the location of this point. In general it is true that the precipitation should be distributed along the trajectory but the difficulties in doing this correctly are insurmountable with a 12-hour time step. The retention of the precipitable water past the saturation point should also lead to excessive values of W' at the end of the trajectory because of the exponential growth rate due to the vertical motion.

A solution to this problem is the use of shorter time steps. It is not practical to test this procedure using observed values since the observation cycle is twelve hours. It could be done using forecasted values of steering flow in time steps as short as one hour. However, this is beyond the scope of the present investigation.

V. DISCUSSION OF RESULTS

In the evaluation of the three forecasts that were made it is of interest to keep in mind the vertical resolution that it is hoped the two-layer model will give. How well the stratification of moisture is forecast is evident from the comparison between predicted values of the precipitable water and relative humidity and the observed values. As an aid in showing this separation, the areas of forecast precipitation are distinguished according to source layer.

The configuration and magnitude of the moisture pattern in the 12-hour forecast valid at 1200 GMT January 8, 1965 (Figs. 12 and 13) shows general agreement with the observed pattern (Figs. 17 and 18). The results along the Oregon-Northern California coast and the Gulf coast are less successful than those elsewhere, due in large part to the origination of trajectories over bodies of water where the initial distribution of moisture was unknown. This source of error is inherent in all the forecasts. In the Great Basin and lower west coast areas a slight drying out of the air was forecast and observed in the lower layer as the surface high pressure cell extended into the region. The increase in moisture over the eastern third of the country was well forecast. Some of this increase is due to the advection of more moist air from the southwestern part of the region, and the persistent upward vertical motion during the 12-hour period enhanced the moisture.

In the upper layer forecast the moist tongue extending from Texas through Missouri in advance of the front was somewhat overdeveloped but the decrease in moisture over the warm sector in the central Great Lakes was predicted well.

Turning to the precipitation area forecast (Fig. 14) and the observed 12-hour precipitation (Fig. 16), it is seen that in the east the area where precipitation occurred in the period is fairly well delineated. The grid used is too coarse to give much resolution in the distribution pattern but a maximum value of 1.18 cm was forecast near Syracuse, N. Y. The lower layer contributed .80 cm while the remaining .38 cm fell from the upper layer. Although only .50 cm was observed at this location, over 1.50 cm fell upstream. This agreement is quite good, especially in light of the fact that the effect of the release of latent heat on the precipitation amount is not included in this model. An underestimate of amount is to be expected in this case. Vederman (1961), employing a technique suggested by Smebye (1958) found that the inclusion of this effect could increase the precipitation amount by as much as three times. In this example of stratiform precipitation ahead of the warm front, the large scale diagnostic vertical motion is probably quite representative of the actual field. The precipitation in the Northwest and upper Plains states is generally in good agreement with the observed. The area where the forecast is poorest is along the Continental Divide. Much of the observed precipitation is undoubtedly orographic in nature and the detail of the terrain used in the test may not be sufficient to give this effect. The precipitation forecast in eastern Colorado, however, does give some indication of the moisture available and the maximum observed precipitation is found west of this area. It is only fair to say that due to the smoothed terrain used in the lower layer formulation and the neglect of the terrain effect on the upper layer moisture, the representation of the moisture

distribution in the vicinity of large barriers such as the Continental Divide given by the model may be far from realistic. For purpose of comparison, a 12-hour precipitation area forecast was made using the one-layer "SLY" model of Younkin, LaRue, and Sanders (1965). The resulting pattern (Fig. 15) shows an excessive amount in the central and southern Rockies extending into the plains and in addition expanded the size of the area in the east. The former error is an interesting one and is due chiefly to the fact that the cold push east of the Rockies was limited to the low layers of the atmosphere, casting doubt on the validity of assumptions in the SLY model so far as temperature advection is concerned. The observed thickness change, following the steering flow, for the SLY model was negative in this area, implying ascent and resulting in a large precipitation area. The occurrence of this ascent is, however, questionable. The discrepancies in the east and along the Rockies are probably due in part to the assumption of saturation at 70% relative humidity. It must be pointed out, however, that the precipitation area in western Colorado and northern New Mexico were well forecasted. In summary it appears that the precipitation area forecast by the two-layer model was somewhat superior to that of the single-layer model.

In the forecasts verifying at 0000 GMT January 9, 1965 (Figs. 21, 22, 23, 24, 25, and 26), there is an area in the southeast where excessive moisture is forecast in the lower layer in both the 12-hour and the 24-hour forecasts. In the latter case this is due in part to excessive values used as initial conditions. The remaining error may be due to unrepresentativeness of the large scale

diagnostic vertical velocities. It is noted that a large area in the southeast extending from Mississippi through Kentucky and eastward to the coast experienced a decrease in moisture during the 12-hour period that cannot be explained by advection. Throughout most of the area the large scale vertical motion is given as slight ascent although descent appears to be required for the proper moisture field to result.

The upper layer 24-hour forecast displayed an excess of precipitable water in the middle of the country where the 0.50 cm isopleth in particular extended too far northward into the plains. The reason for this excess is probably the erroneous initial conditions used. The observed distributions are shown in Figures 30 and 31. Another area of error on the 24-hour lower-layer forecast was in the lower Great Lakes region where dry air was moved too far eastward. The dryness resulted from the value forecast at one grid point in northern Illinois. The trajectory terminating at that point originated in the somewhat drier air over northern Minnesota. The explanation of this error is not immediately clear. Upward vertical motion was experienced along the entire trajectory and yet there was an increase in the 1000-mb to 700-mb thickness. It is difficult to reconcile the diagnostic vertical velocity with the observed change in thickness which occurred over the trajectory.

The tendency for the axis of maximum moisture to extend into Colorado, on the upper layer forecasts in particular, resulted in part from the contribution of a trajectory which terminated in eastern Colorado. The steering flow in that area was weak in strength and of uncertain direction at both 1200 GMT January 8

and 0000 GMT January 9, 1965. The trajectory constructed in the flow gave an originating point in the relatively moist air to the south of the subject grid point.

In general the discrepancies between the forecast and the actual observed values of precipitable water can be explained by uncertainty of trajectories or, in the case of the coastal points, by the lack of moisture information at the upstream point. Much of the error in precipitation area forecasts was due to uncertainty of trajectories and to the difficulty of treating trajectories which cross large mountain barriers. In this study only the elevation of the initial and the terminal points of trajectories were considered in arriving at the orographic effect but it is possible that the elevation at some intermediate point was of greater importance.

In the east too large a southward extension of precipitation was forecast from a low layer source in the 24-hour forecast. The 12-hour forecast essentially corrected this error reflecting the influence of using actual precipitable water for input data.

Of particular interest in the precipitation forecasts was the detection of the precipitation area which developed in the central part of the country between 1200 GMT January 8 and 0000 GMT January 9. The forecast suggests an upper layer source for the precipitation and a check of individual upper air soundings in the region of the precipitation tends to bear this out. The soundings at Columbia, Mo. (445) at 1200 GMT, just before the beginning of the rainfall, and at Topeka, Kan. (456) and Ft. Worth, Texas (259) at 0000 GMT, after the

beginning of the precipitation (Fig. 32) show a low level dry layer topped by a relatively moist layer at higher altitudes. Any precipitation originating in these air masses must have had its source in a layer roughly equivalent to our 700-mb to 500-mb layer. For a group of stations including Columbia, Mo. (445), Peoria, Ill. (532), Topeka, Kan. (456), and Oklahoma City (353) the ratio of the precipitable water in the lower later to the precipitable water in the upper layer decreased from 4 to 1 at 0000 GMT January 8 to 2 to 1 at 0000 GMT January 9. This was a clear indication of the change in the relative moisture content of the two layers during the forecast period. The lower layer over the central Mississippi valley showed noticeably more moisture than forecast at 0000 GMT January 9 but it seems likely that this increase resulted from the evaporation of moisture falling through the layer from an upper source. The forecast model, it must be remembered, does not account for evaporation.

The model also handled fairly well cases of low level moisture and upper dryness. The sounding for Jackson, Miss. (235) is shown as an example (Fig. 32). While the forecast relative humidities are somewhat lower than those that occurred, the delineation of the moisture by layer is clearly indicated.

The separation of moisture across the central United States which developed by 0000 GMT January 9 was predicted quite well, as were the strong gradients of moisture in both forecasts. This resolution is not possible in a single-layer model and it is reassuring to note that the separation was in general agreement to that which occurred.

VI. CONCLUSIONS AND RECOMMENDATIONS

On the basis of the results of this investigation the feasibility of utilizing a two-layer model for the objective prediction of moisture distribution has been demonstrated. That the degree of vertical resolution which is given by this model is realistic has been shown in the limited testing. The moisture stratification observed in the atmosphere during a period of substantial change was successfully reproduced by this forecast model. Although no statistical evaluation was made, subjective verification indicated a high degree of success in the three test forecasts. As a result of a single comparison with a one-layer integrated moisture model, it appears that although the differences were small, the added resolution of the two-layer formulation results in a better forecast.

It was stated at the outset of the derivation that the success of the model was dependent on the goodness of the modeling approximations of the profiles of specific humidity, wind, horizontal divergence, and vertical motion. It is obvious that the most appropriate modeling parameters must be used. To this end, variations such as those noted in this study with respect to the β profile should be carefully evaluated. The use of monthly or seasonal values if significant variations are persistent should be investigated, as should the use of regional values for those functions which have a well-defined areal variability.

Another field of inquiry which demands further study is that of the effect of the underlying terrain on the moisture transport. Of particular

importance to this model is the proper treatment of trajectories which cross mountain barriers. The relationship between the moisture parameters and the percentage and type of cloudiness in each layer should be studied to give further usefulness to this forecast model.

It is immediately apparent that additional testing of this model is required before more claims can be made for its success. Forecasts using predicted fields with time steps of six hours or less would give an excellent basis for the evaluation of this model as an operational tool.

BIBLIOGRAPHY

Benton, G. S., and M. A. Estoque, 1954: Water vapor transfer over the North American continent. J. Meteor., 11, 462-477.

Berkofsky, L. and E. A. Bertoni, 1955: Mean topographic charts for the entire earth. Bull. Amer. Meteor. Soc., 36, 350-354.

Carlstead, E. M., 1959: Forecasting middle cloudiness and precipitation areas by numerical methods. Mon. Wea. Rev., 87, 375-381.

Smagorinsky, J. and G. O. Collins, 1955: On the numerical prediction of precipitation. Mon. Wea. Rev., 83, 53-68.

Smebye, S. J., 1958: Computation of precipitation from large-scale vertical motions. J. Meteor., 15, 547-560.

Staff Members in Tokyo University, 1955: The quantitative forecast of precipitation with the numerical method. J. Meteor. Soc. Japan, 33, 204-216.

Vederman, J., 1961: Forecasting precipitation with the aid of a high-speed electronic computer. Mon. Wea. Rev., 89, 243-250.

Younkin, R. J., J. A. LaRue, and F. Sanders, 1965: The objective prediction of clouds and precipitation using vertically integrated moisture and adiabatic vertical motions. J. Appl. Meteor., 4, 3-17.

APPENDIX

	K_1				K_3			
	Jan	Apr	Jul	Oct	Jan	Apr	Jul	Oct
Caribou	.50	.49	.47	.51	.56	.41	.57	.54
Columbia, Mo.	.46	.59	.34	.34	.54	.57	.67	.55
Denver	.54	.56	.35	.62	.48	.55	.70	.52
International Falls	.45	.62	.53	.49	.61	.57	.58	.51
Lake Charles	.65	.49	-2.13	.45	.58	.53	.42	.77
Oakland	.40	.51	.12	.52	.62	.59	.61	.53
Pittsburgh	.53	.46	.53	.43	.55	.62	.48	.60
Spokane	.39	.45	.64	.43	.53	.55	.56	.59
Tampa	.68	.76	-2.14	.89	.62	.59	.89	.64
Tucson	.97	.66	.16	.80	.59	.55	.68	.60
Average	.57	.60	.37	.55	.57	.57	.59	.59

Table 1. - Values of K_1 and K_3 by station and by season.

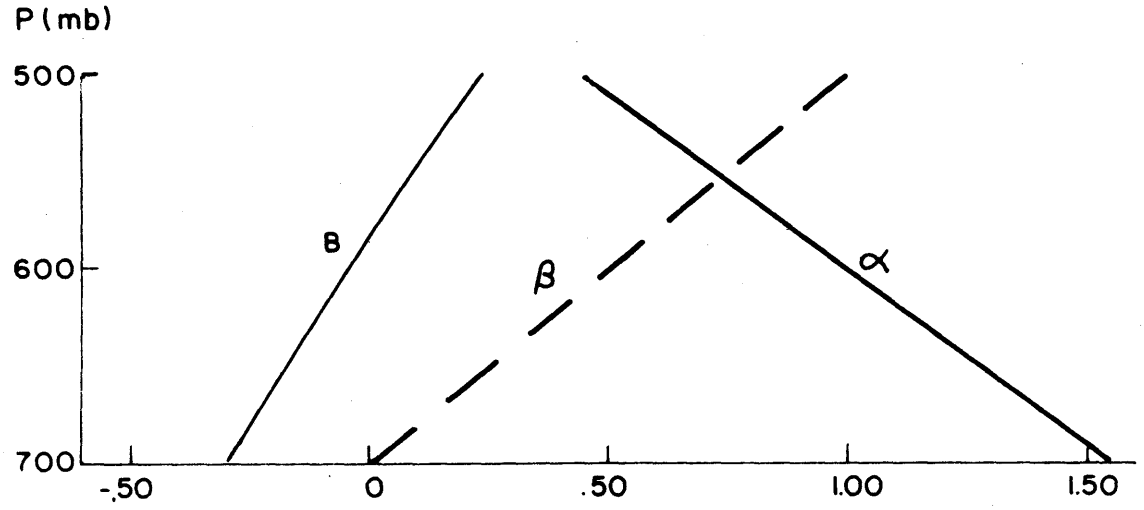

(a) Upper Layer

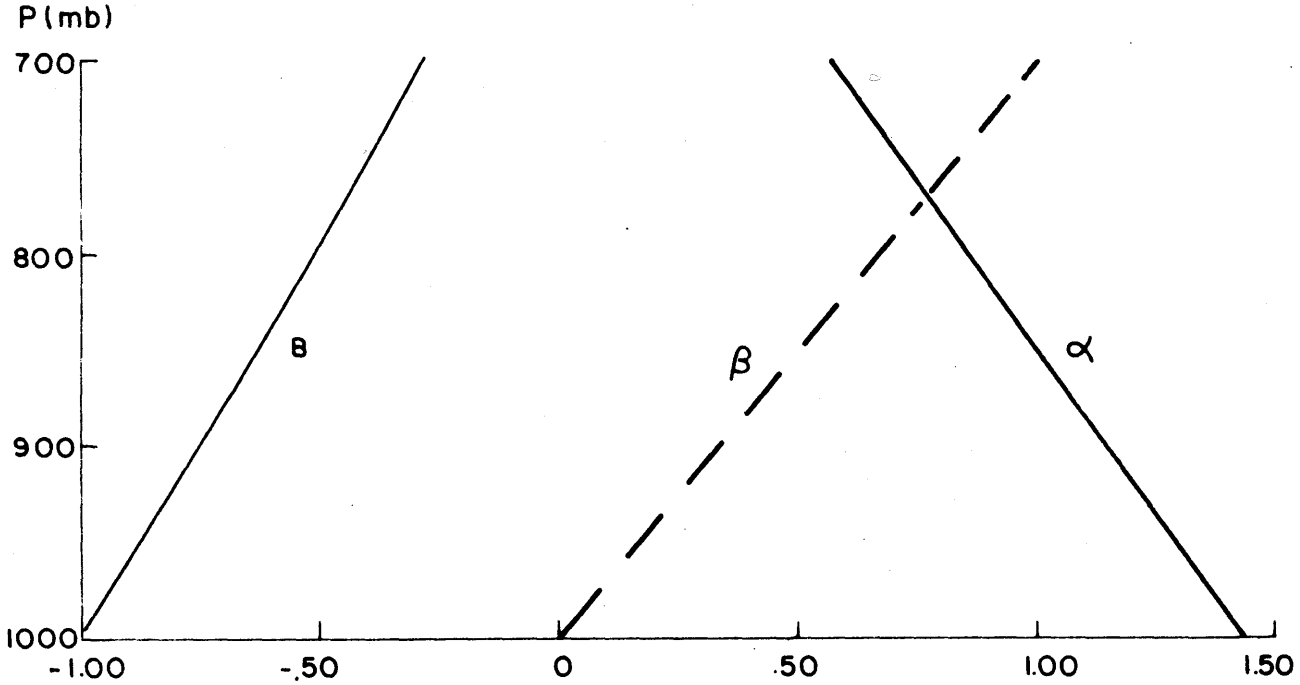

(b) Lower Layer

Fig. 1. Profiles of α, β, and B, the modeling parameters for specific humidity, wind and divergence.

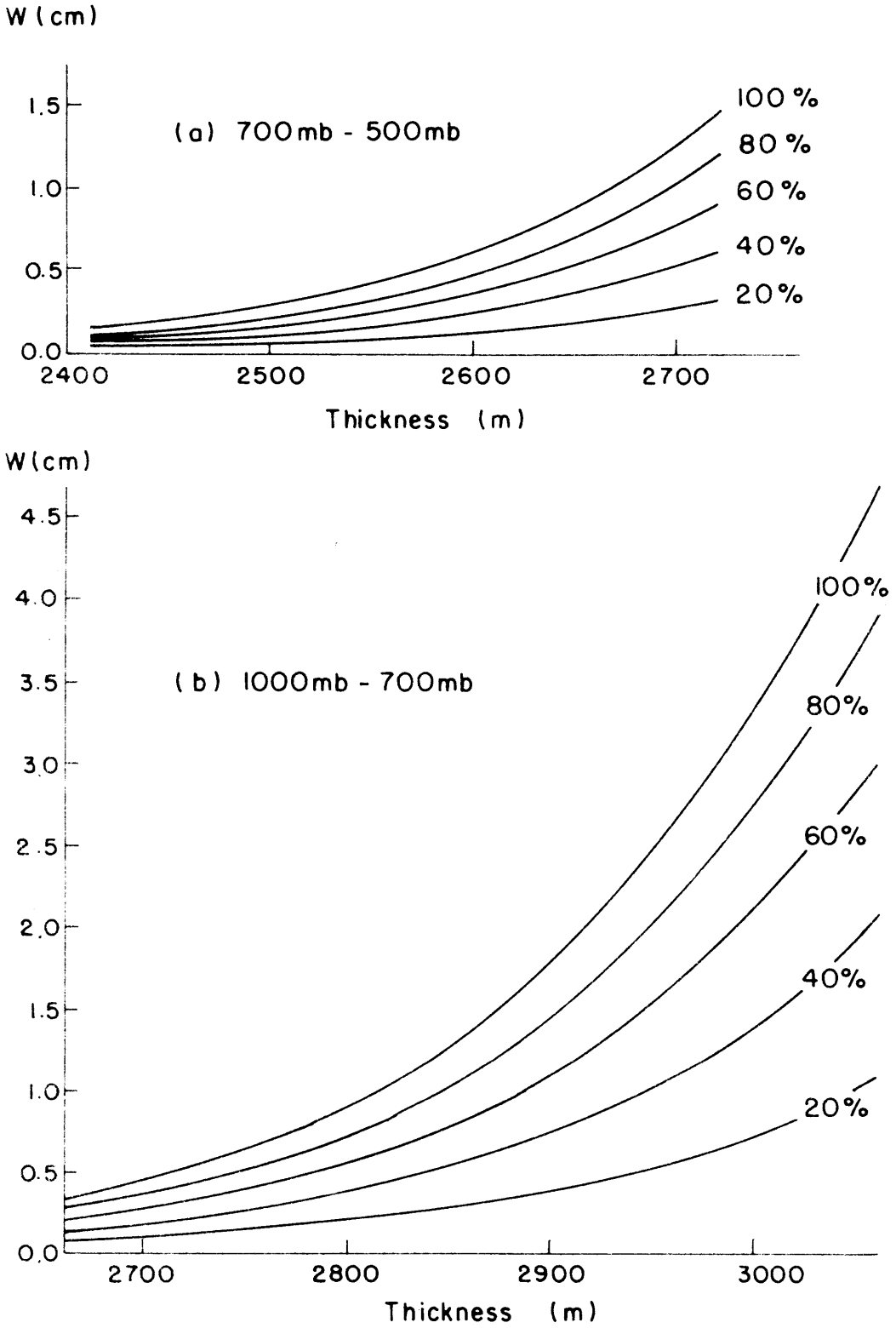

Fig. 2. Relation between thickness, precipitable water, and $\bar{U}$ (approximate mean relative humidity.)

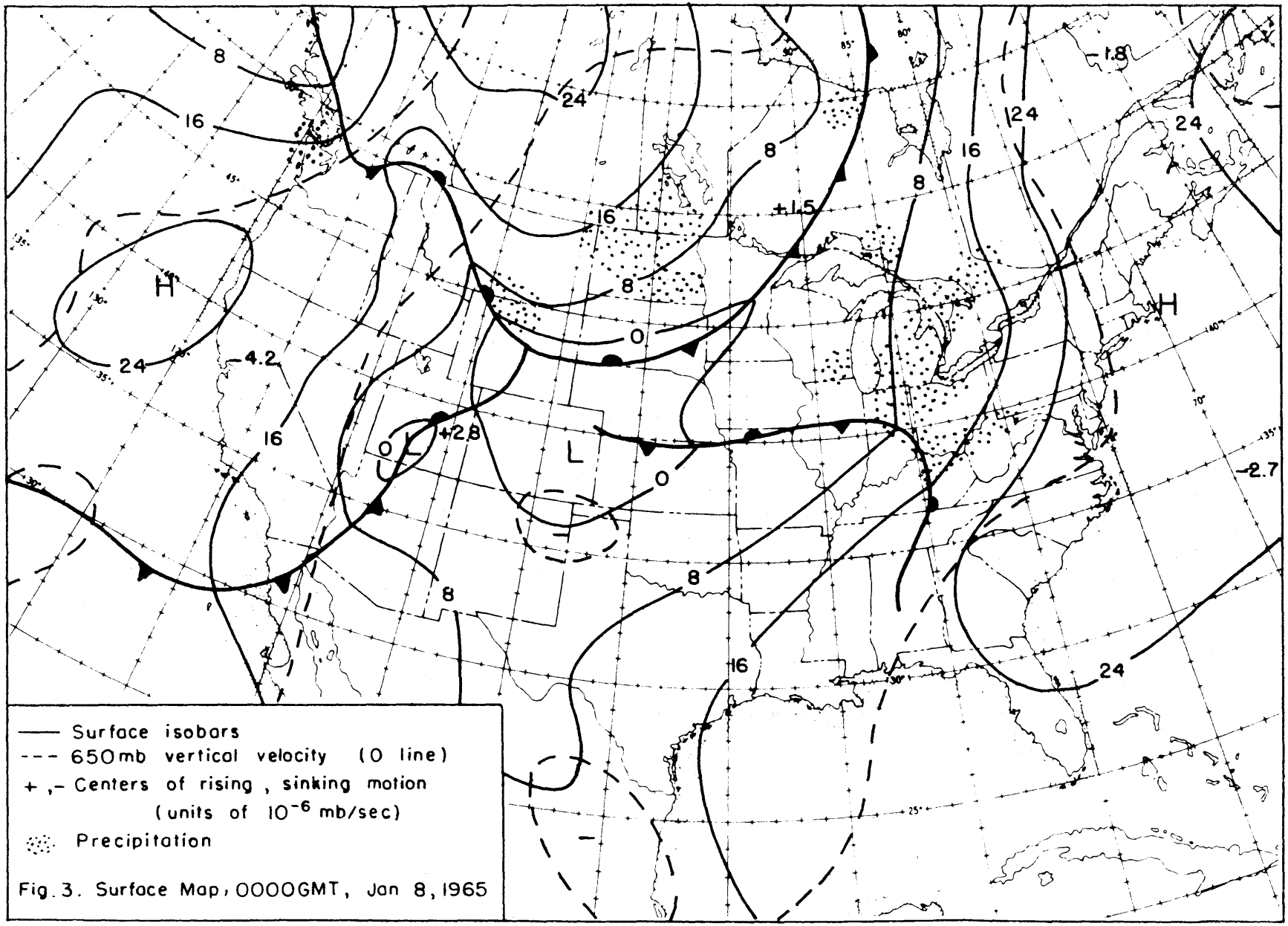

Fig. 3. Surface Map, 0000GMT, Jan 8, 1965

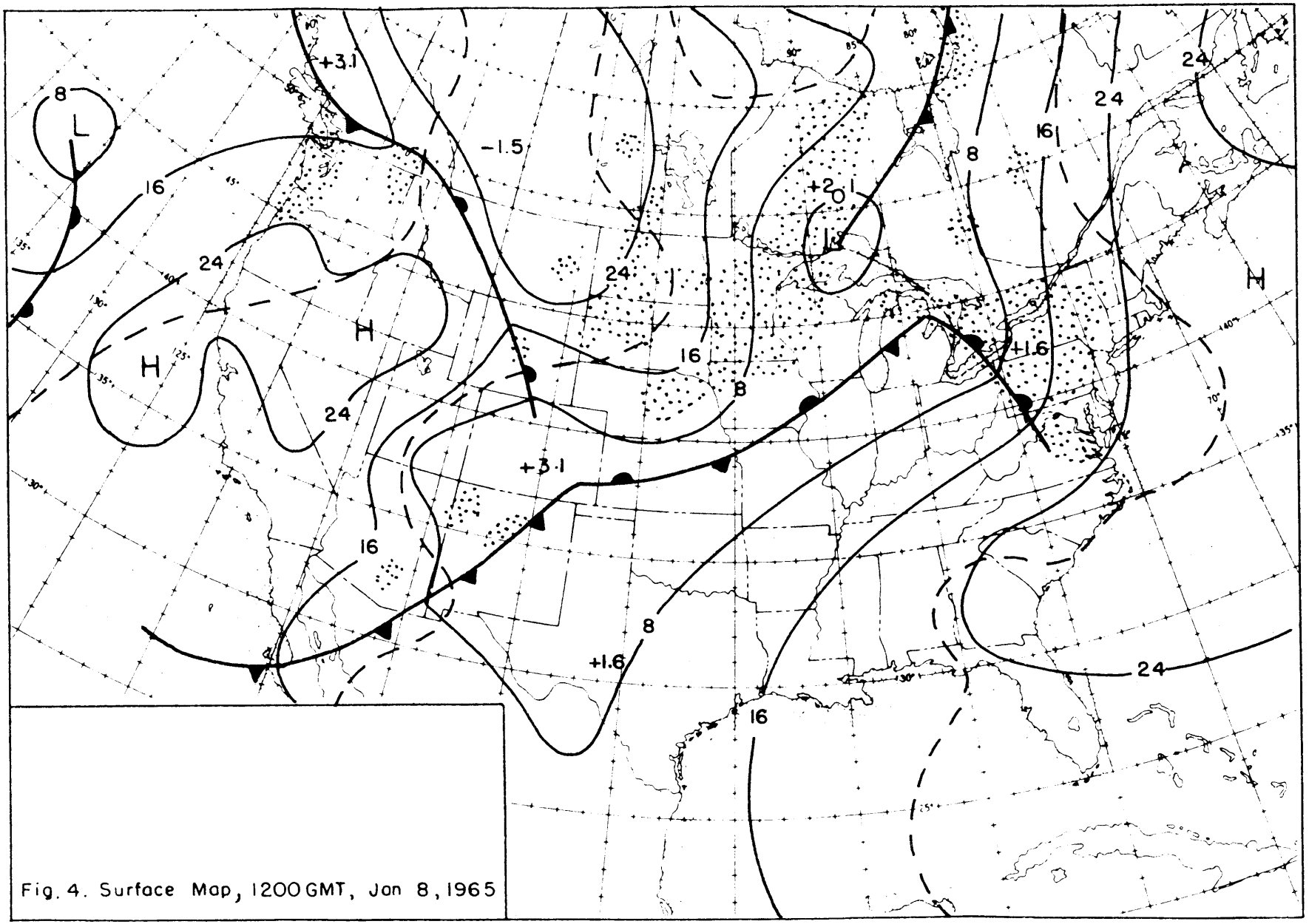

Fig. 4. Surface Map, 1200 GMT, Jan 8, 1965

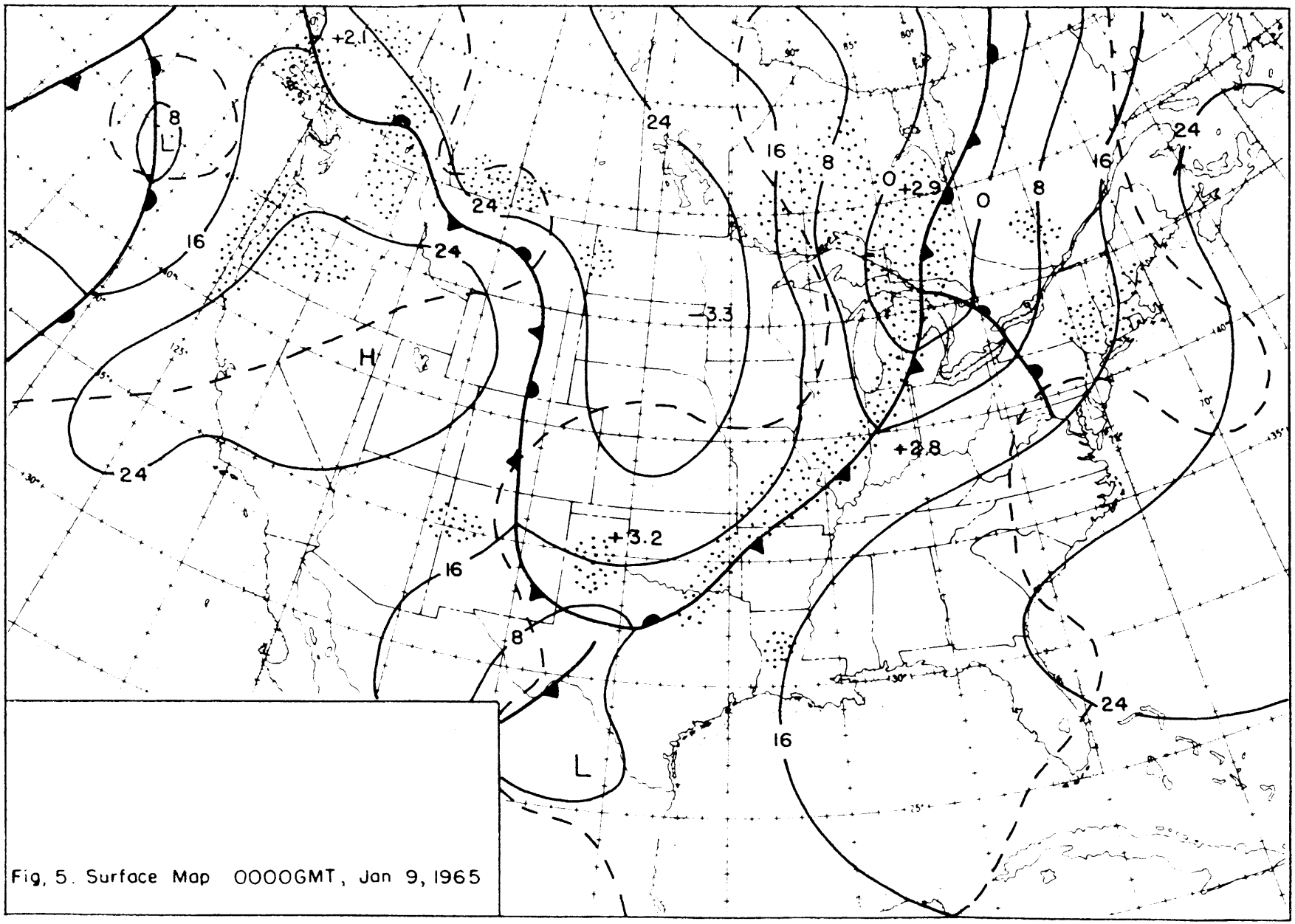

Fig, 5. Surface Map 0000GMT, Jan 9, 1965

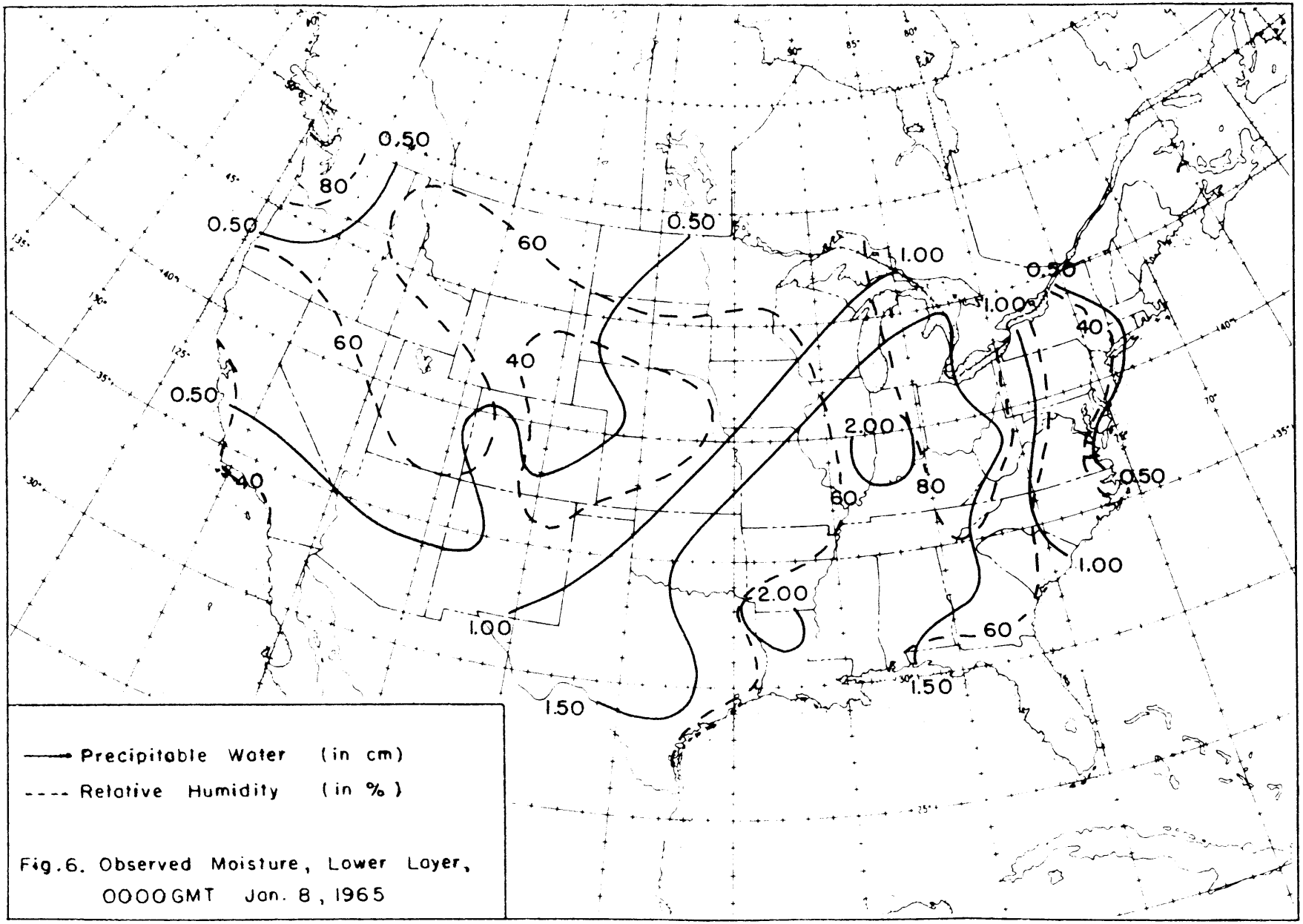

Fig.6. Observed Moisture, Lower Layer, 0000 GMT Jan. 8, 1965

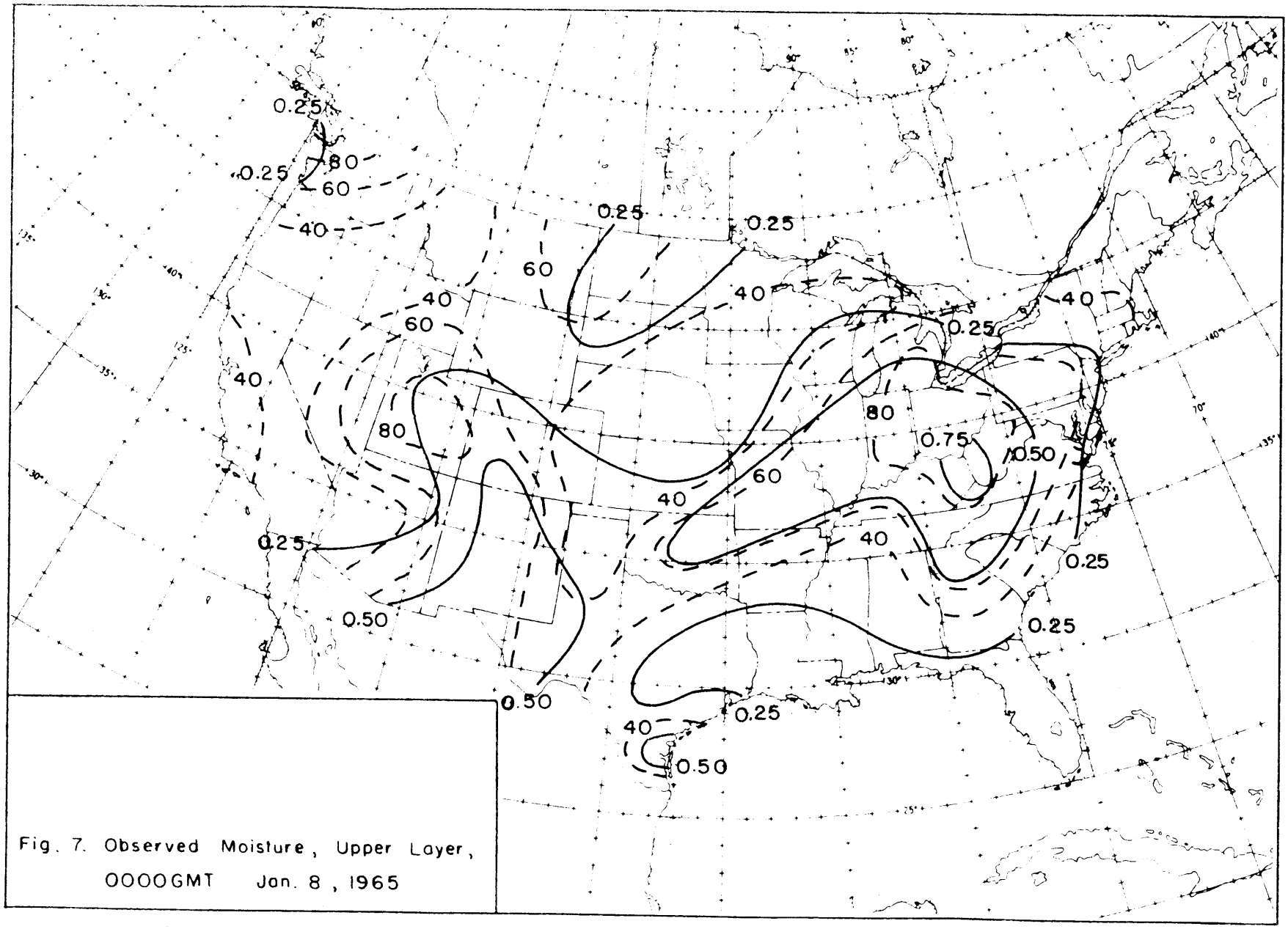

Fig. 7. Observed Moisture, Upper Layer, 0000GMT Jan. 8, 1965

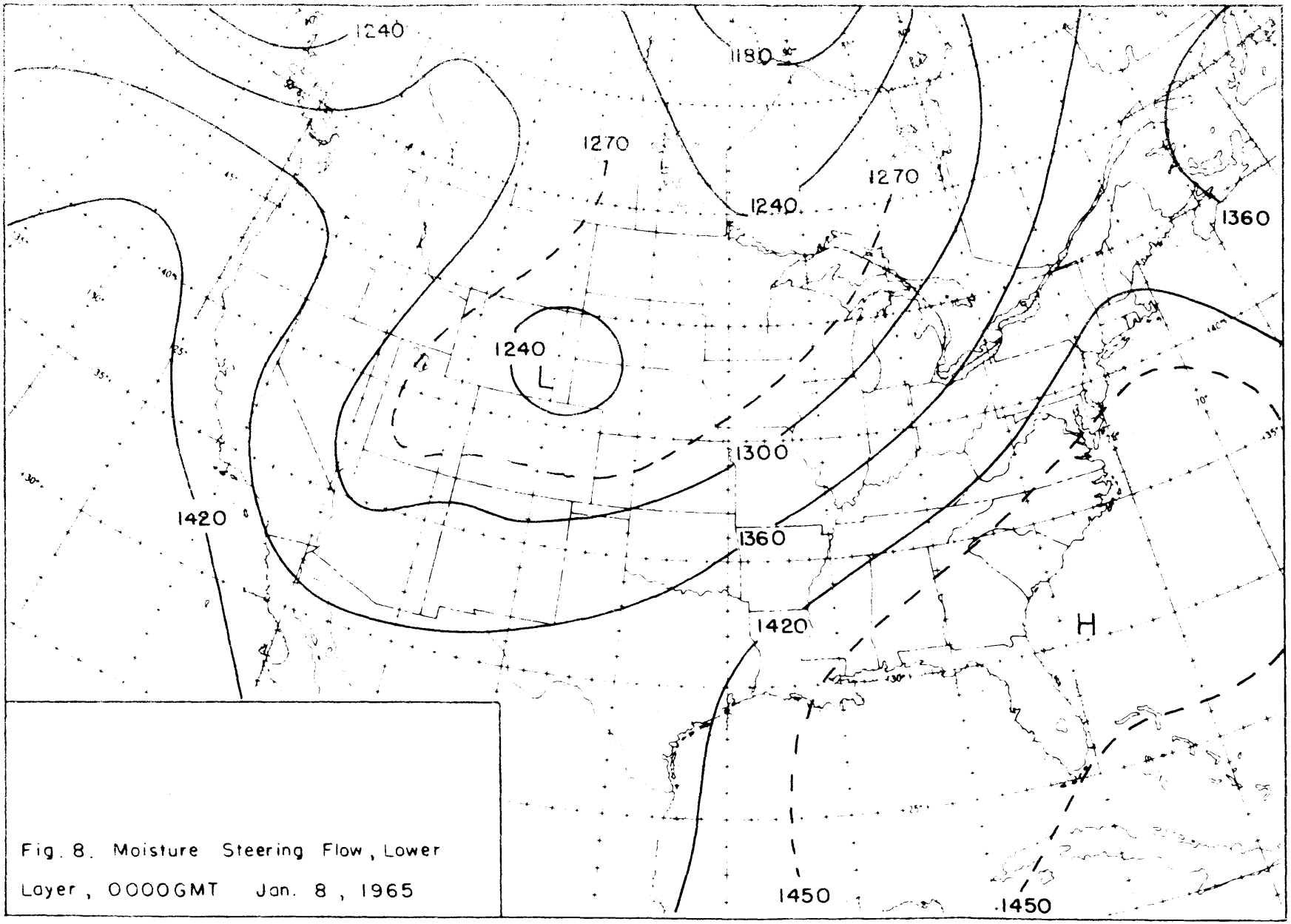

Fig. 8. Moisture Steering Flow, Lower Layer, 0000GMT Jan. 8, 1965

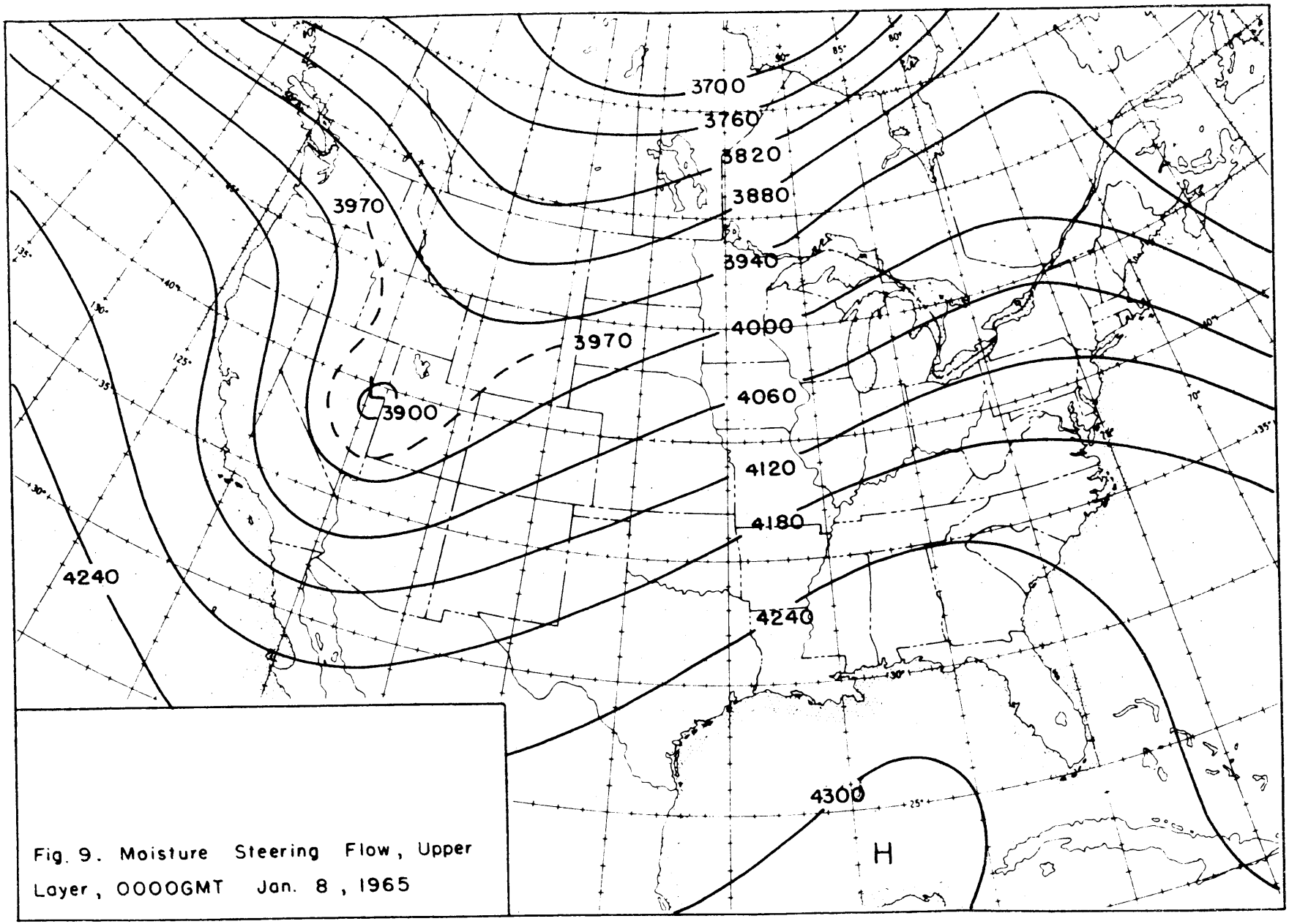

Fig. 9. Moisture Steering Flow, Upper Layer, 0000GMT Jan. 8, 1965

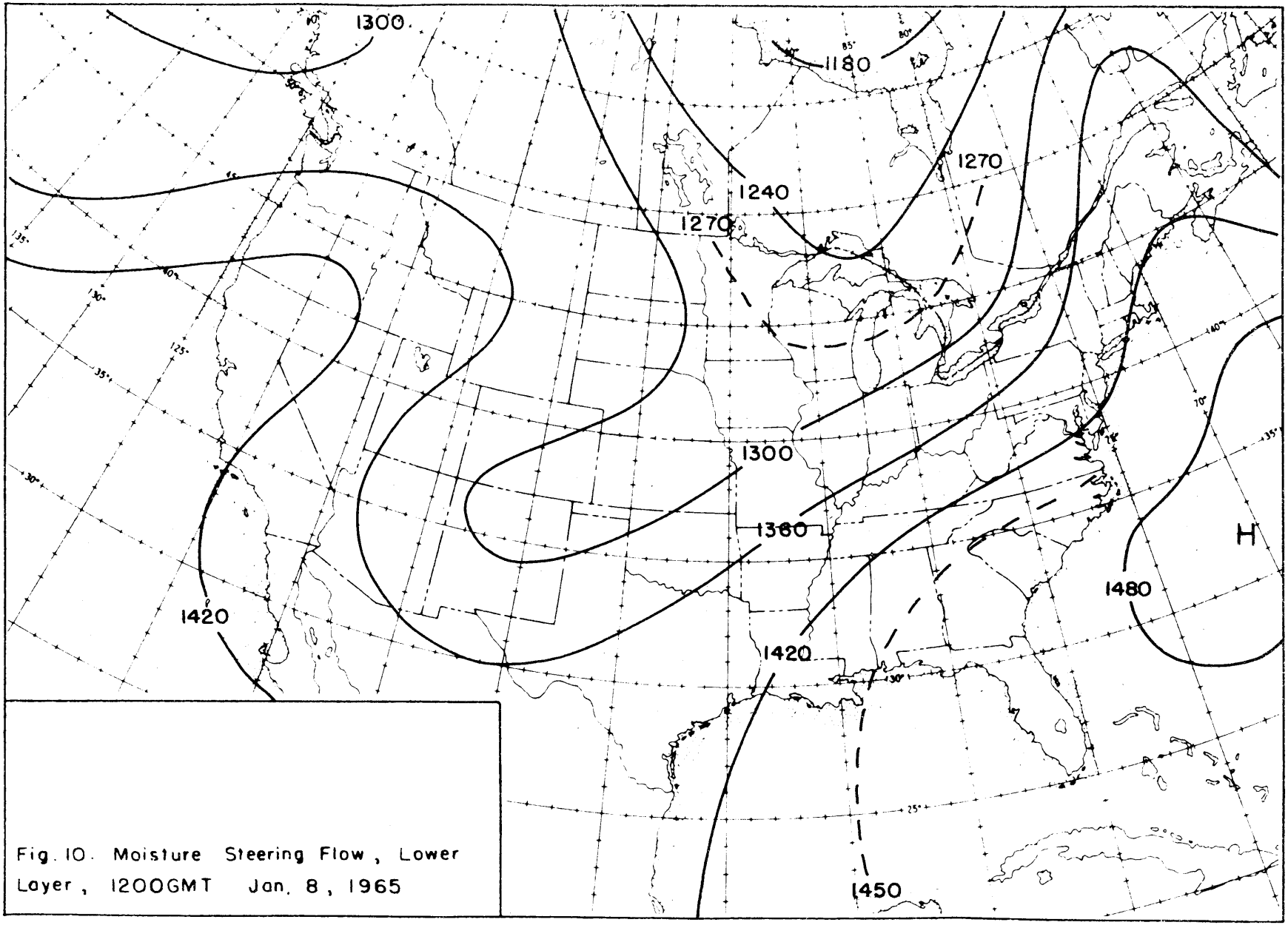

Fig. 10. Moisture Steering Flow, Lower Layer, 1200GMT Jan. 8, 1965

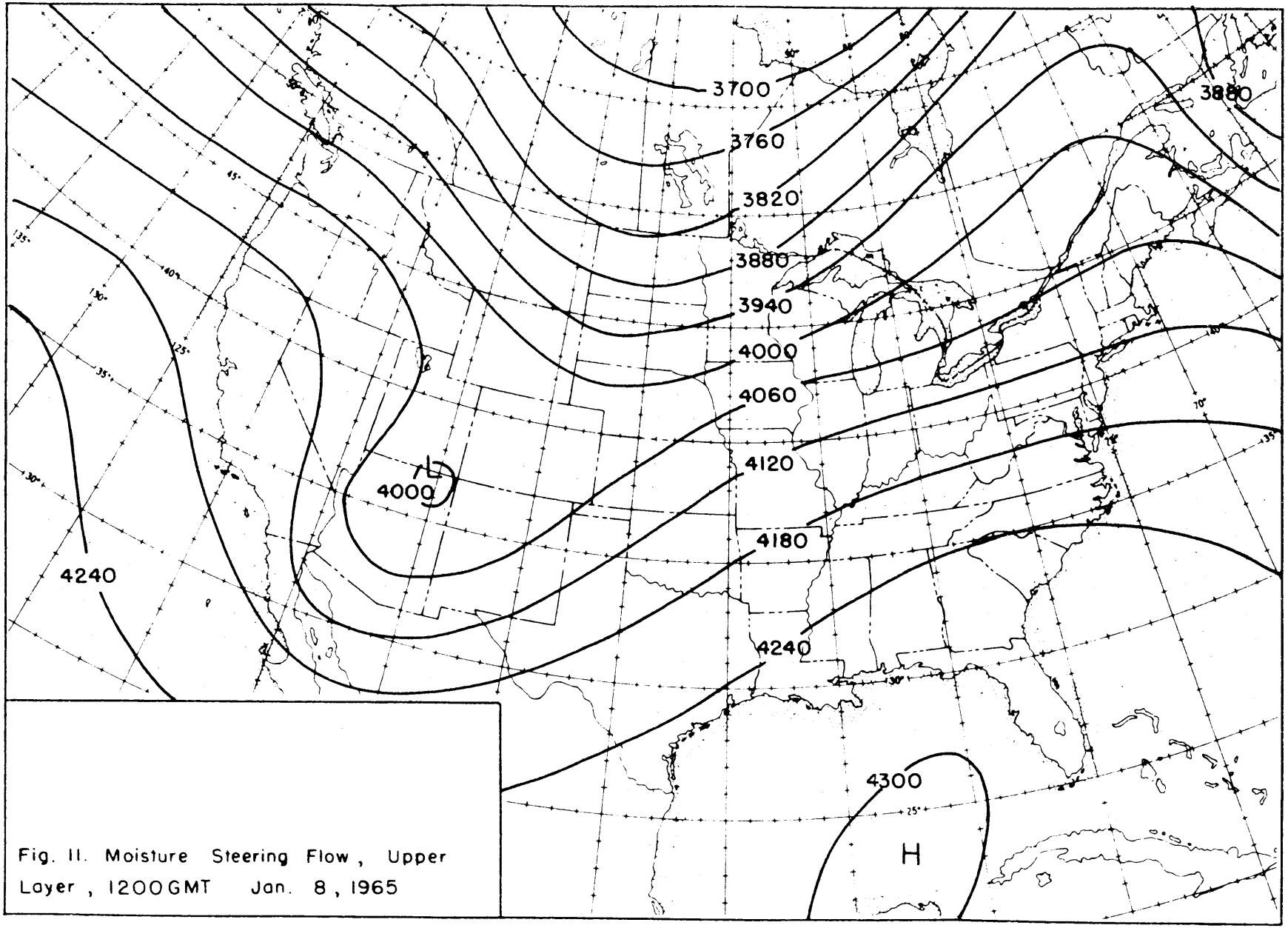

Fig. 11. Moisture Steering Flow, Upper Layer, 1200 GMT Jan. 8, 1965

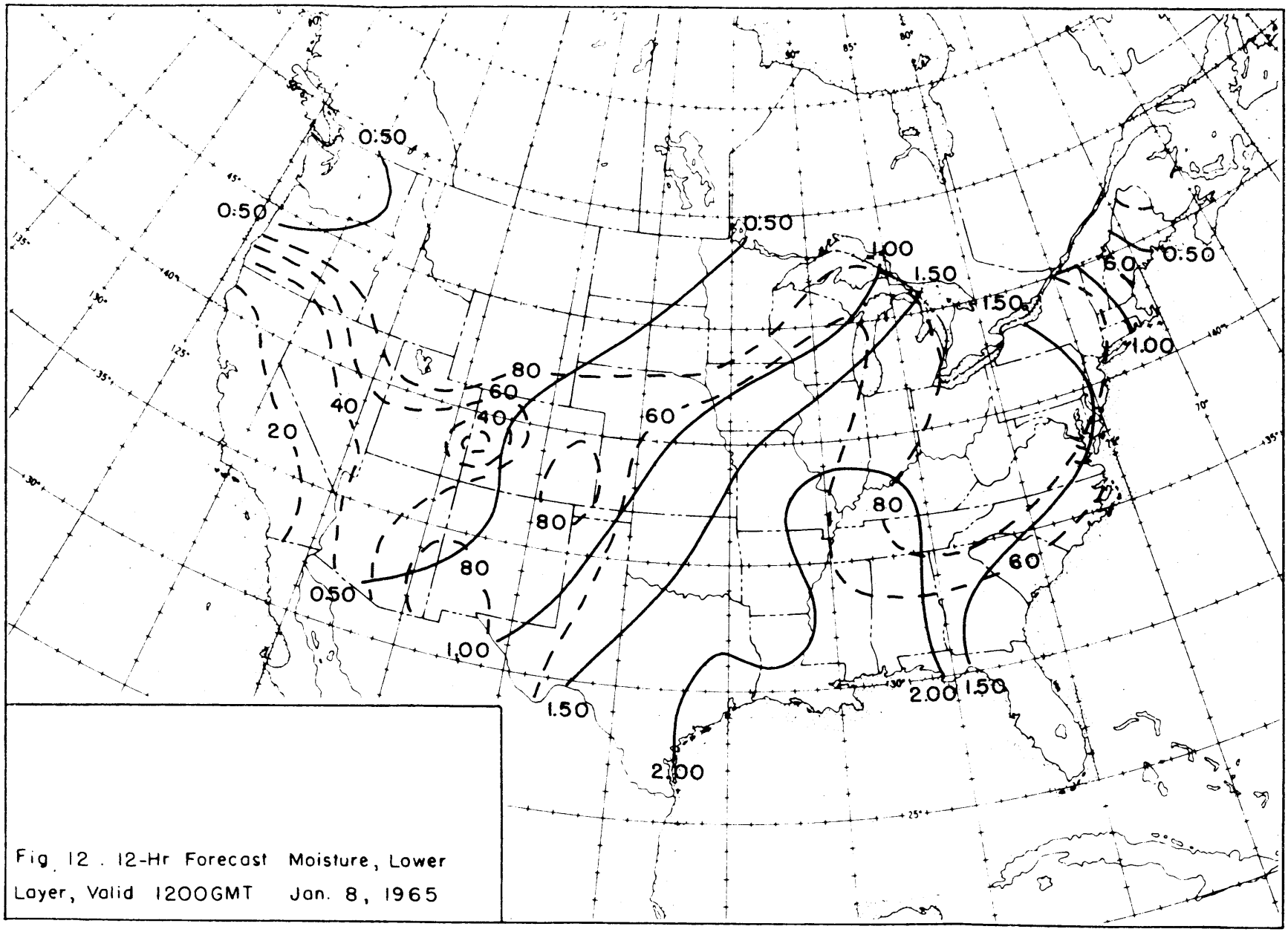

Fig. 12. 12-Hr Forecast Moisture, Lower Layer, Valid 1200GMT Jan. 8, 1965

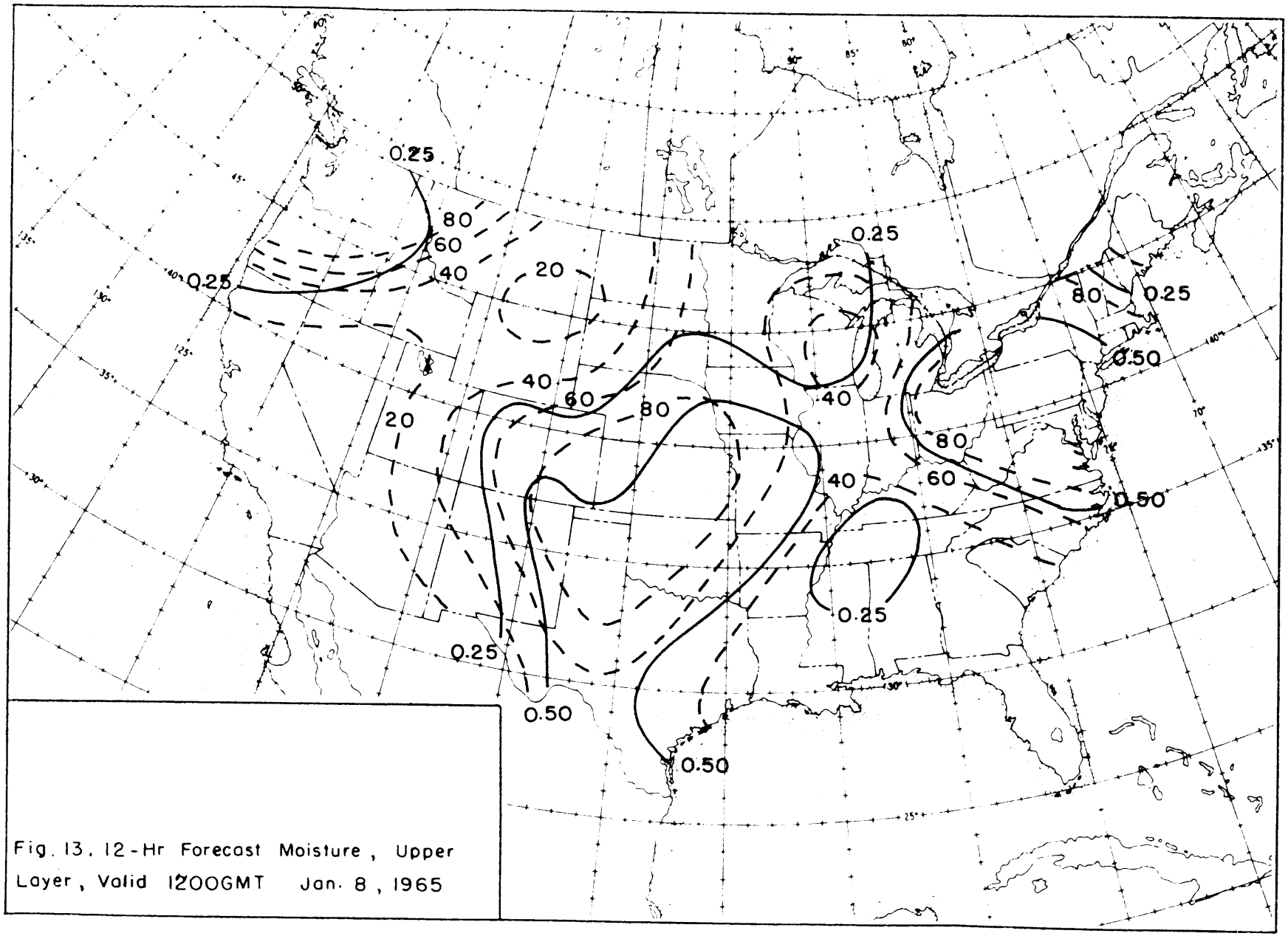

Fig. 13. 12-Hr Forecast Moisture, Upper Layer, Valid 1200GMT Jan. 8, 1965

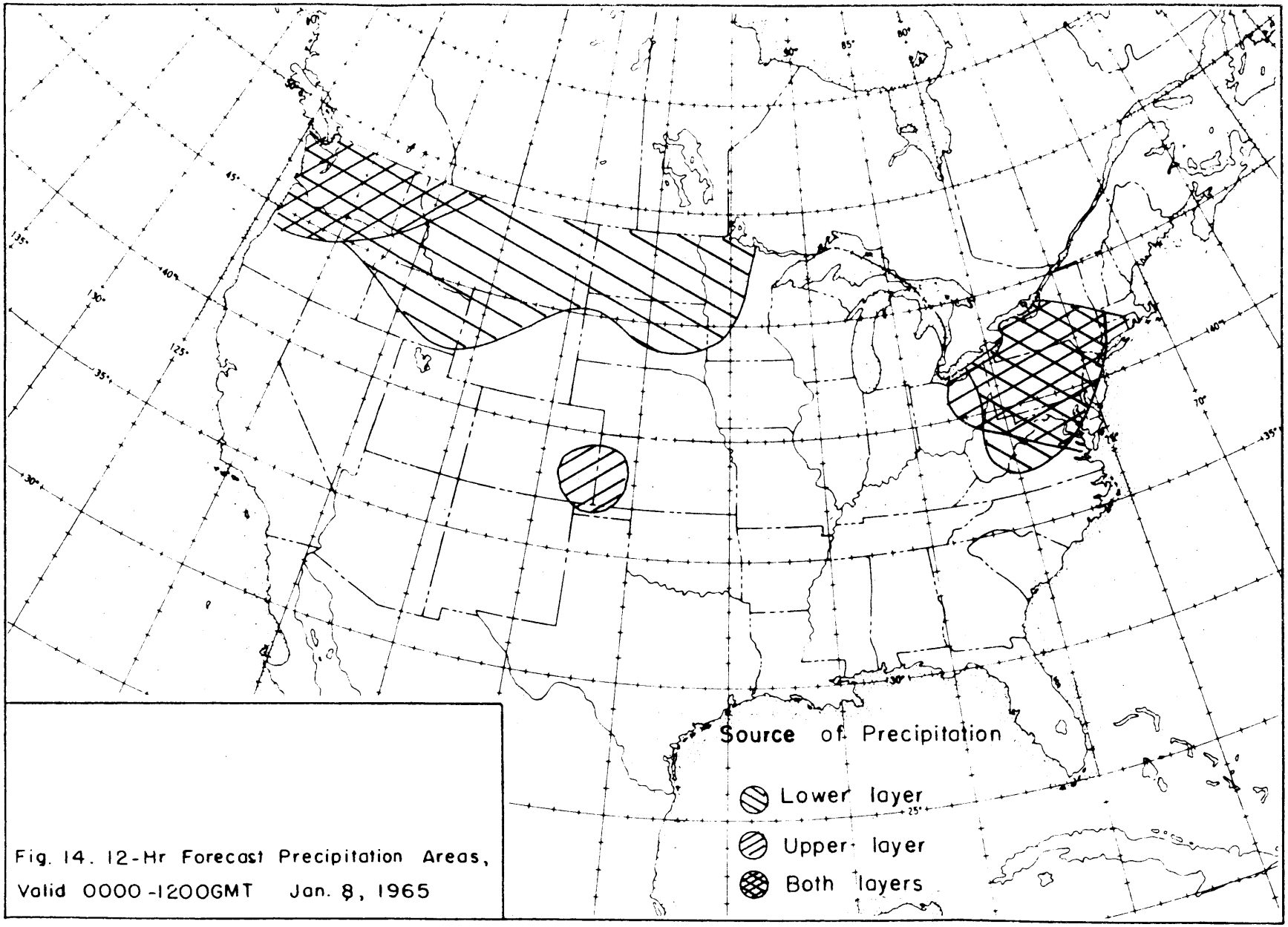

Fig. 14. 12-Hr Forecast Precipitation Areas, Valid 0000-1200GMT Jan. 8, 1965

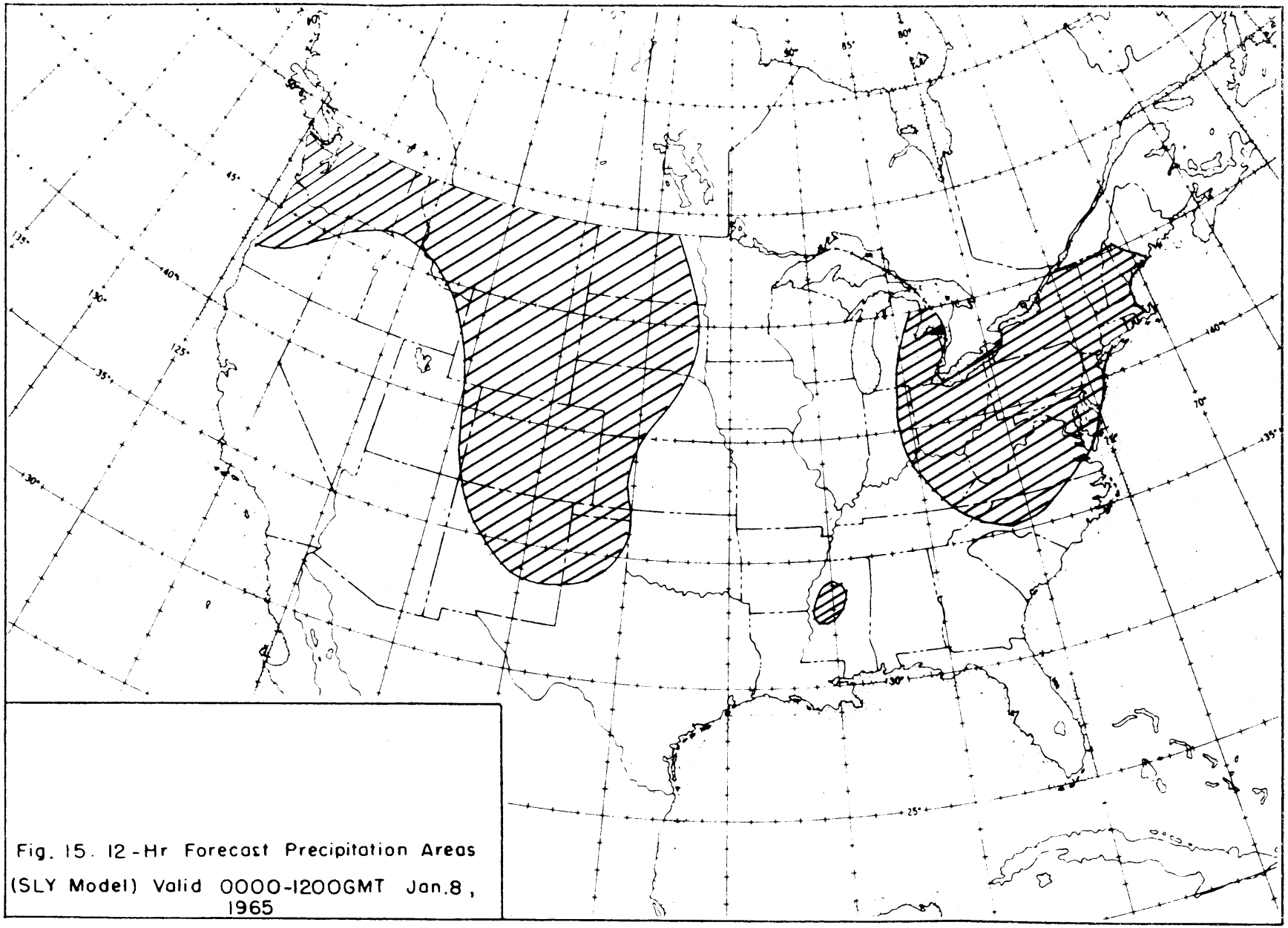

Fig. 15. 12-Hr Forecast Precipitation Areas (SLY Model) Valid 0000-1200GMT Jan.8, 1965

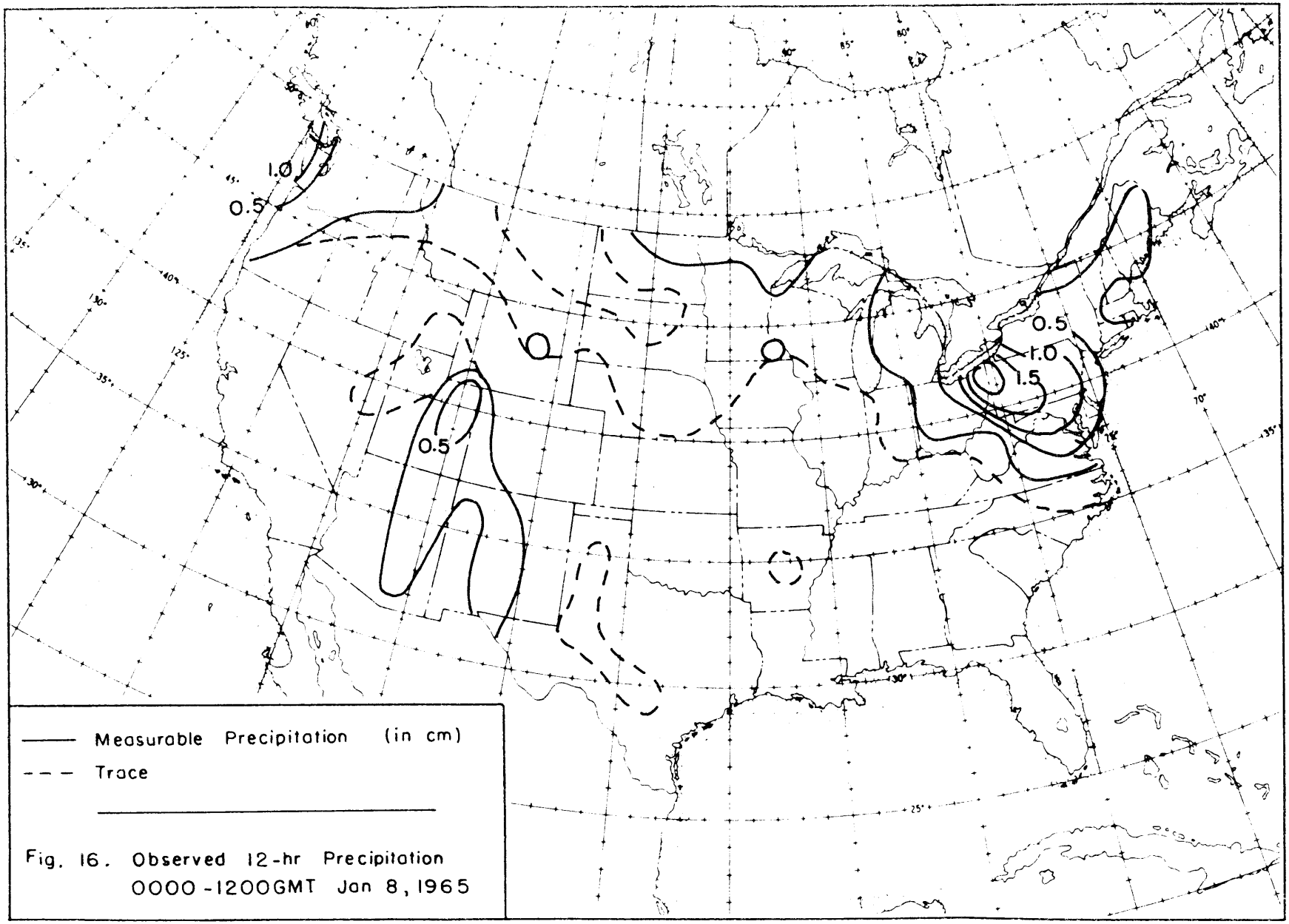

Fig. 16. Observed 12-hr Precipitation
0000-1200GMT Jan 8, 1965

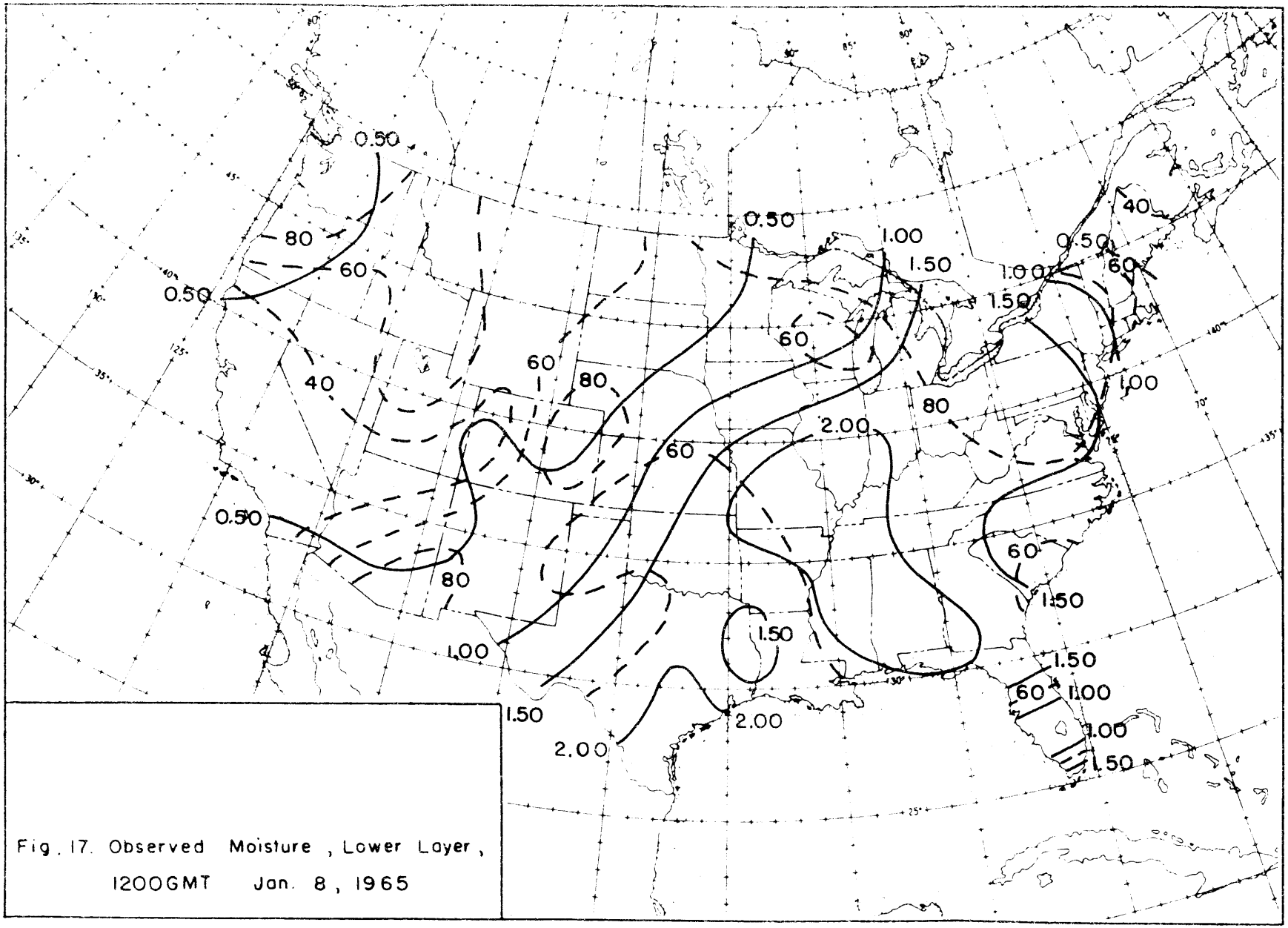

Fig. 17. Observed Moisture, Lower Layer, 1200GMT Jan. 8, 1965

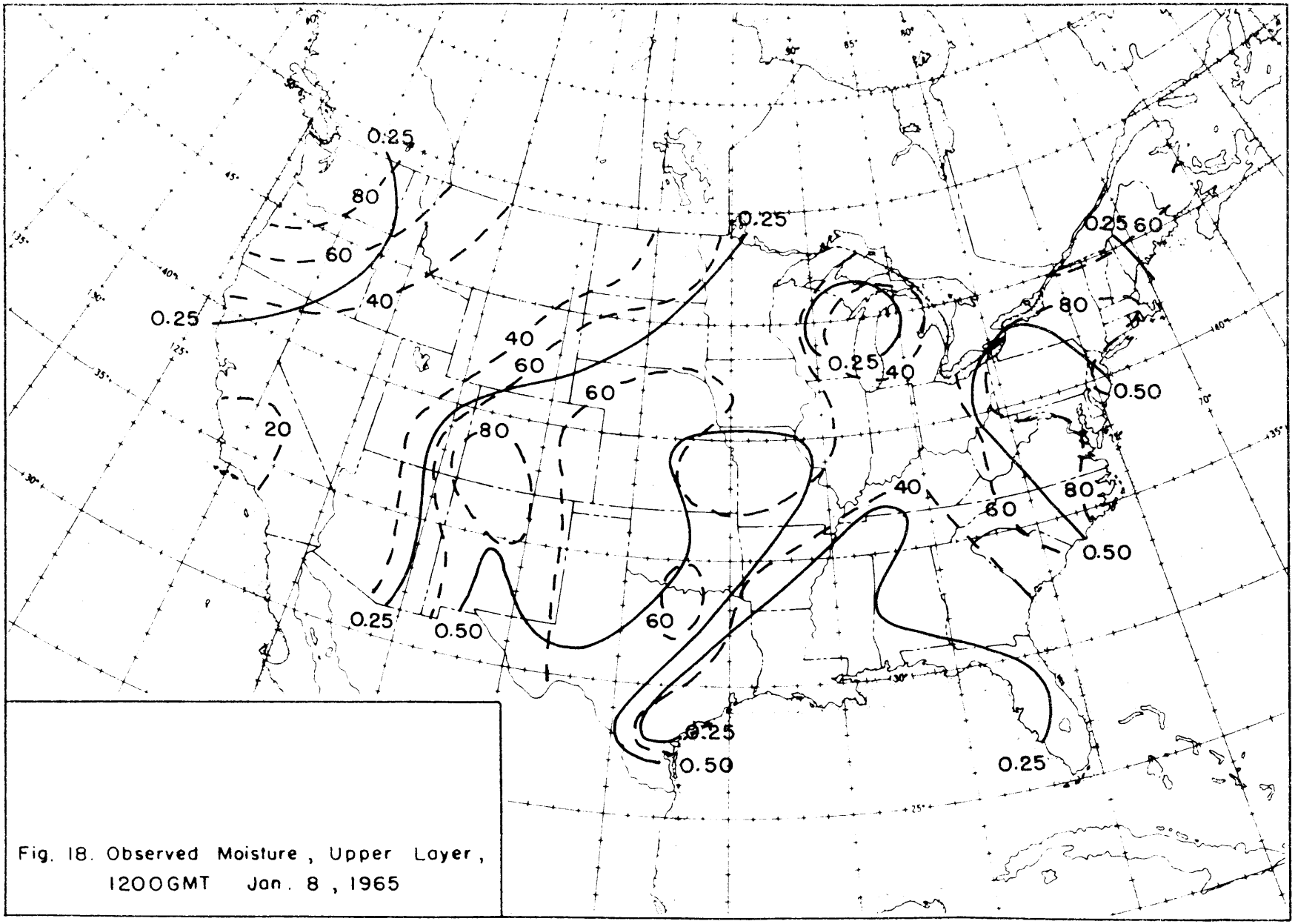

Fig. 18. Observed Moisture, Upper Layer, 1200GMT Jan. 8, 1965

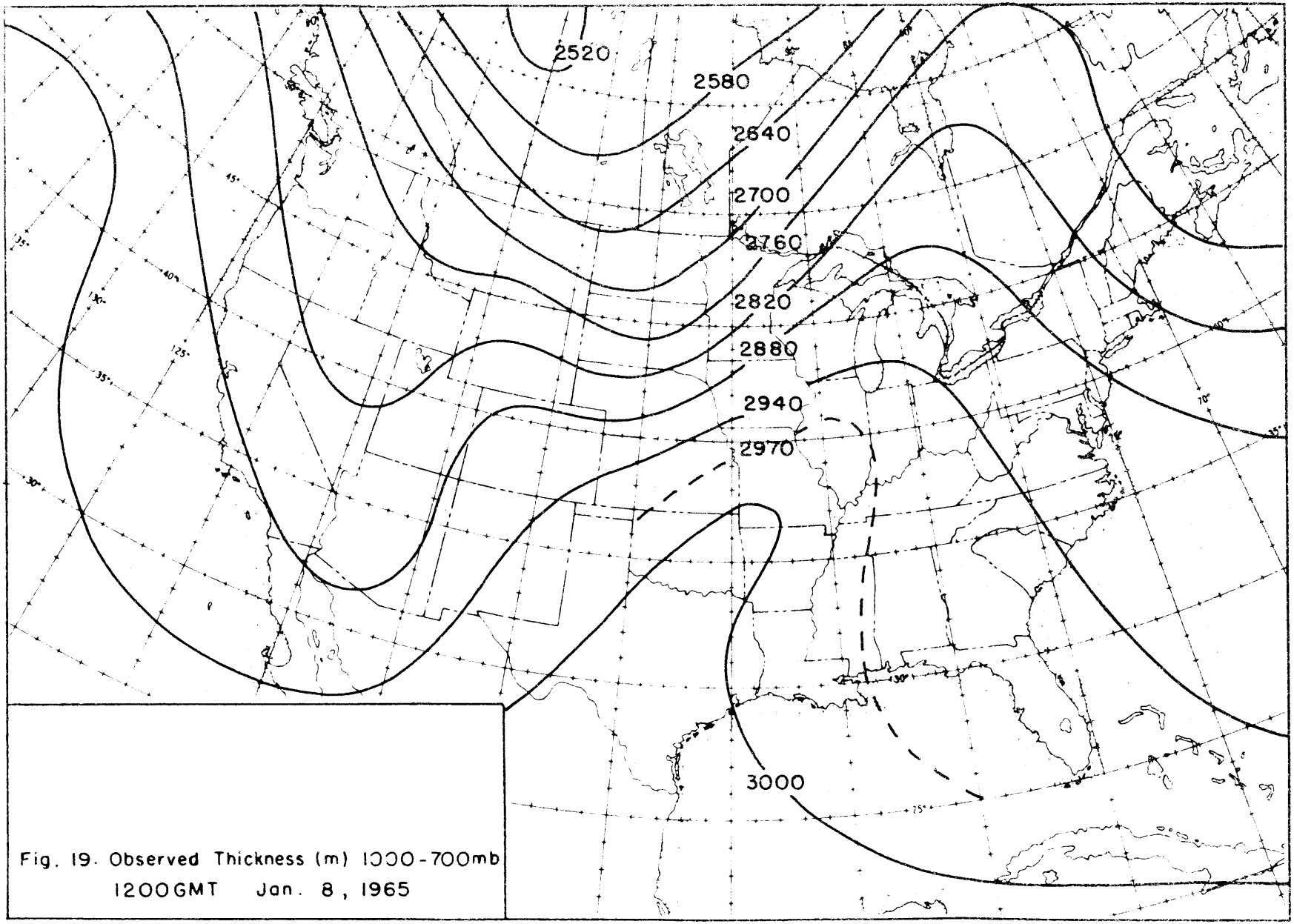

Fig. 19. Observed Thickness (m) 1000-700mb
1200GMT Jan. 8, 1965

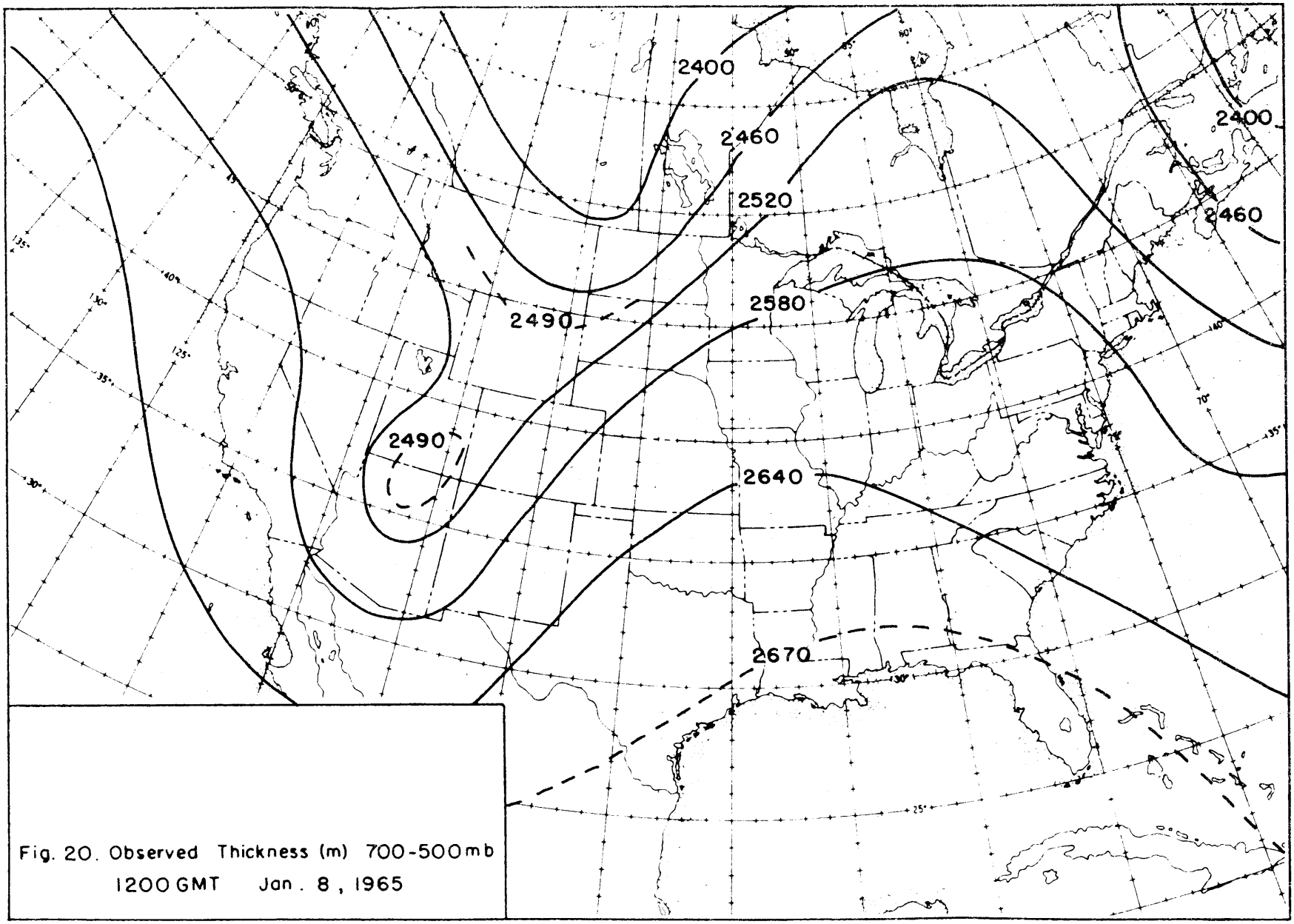

Fig. 20. Observed Thickness (m) 700-500mb
1200 GMT Jan. 8, 1965

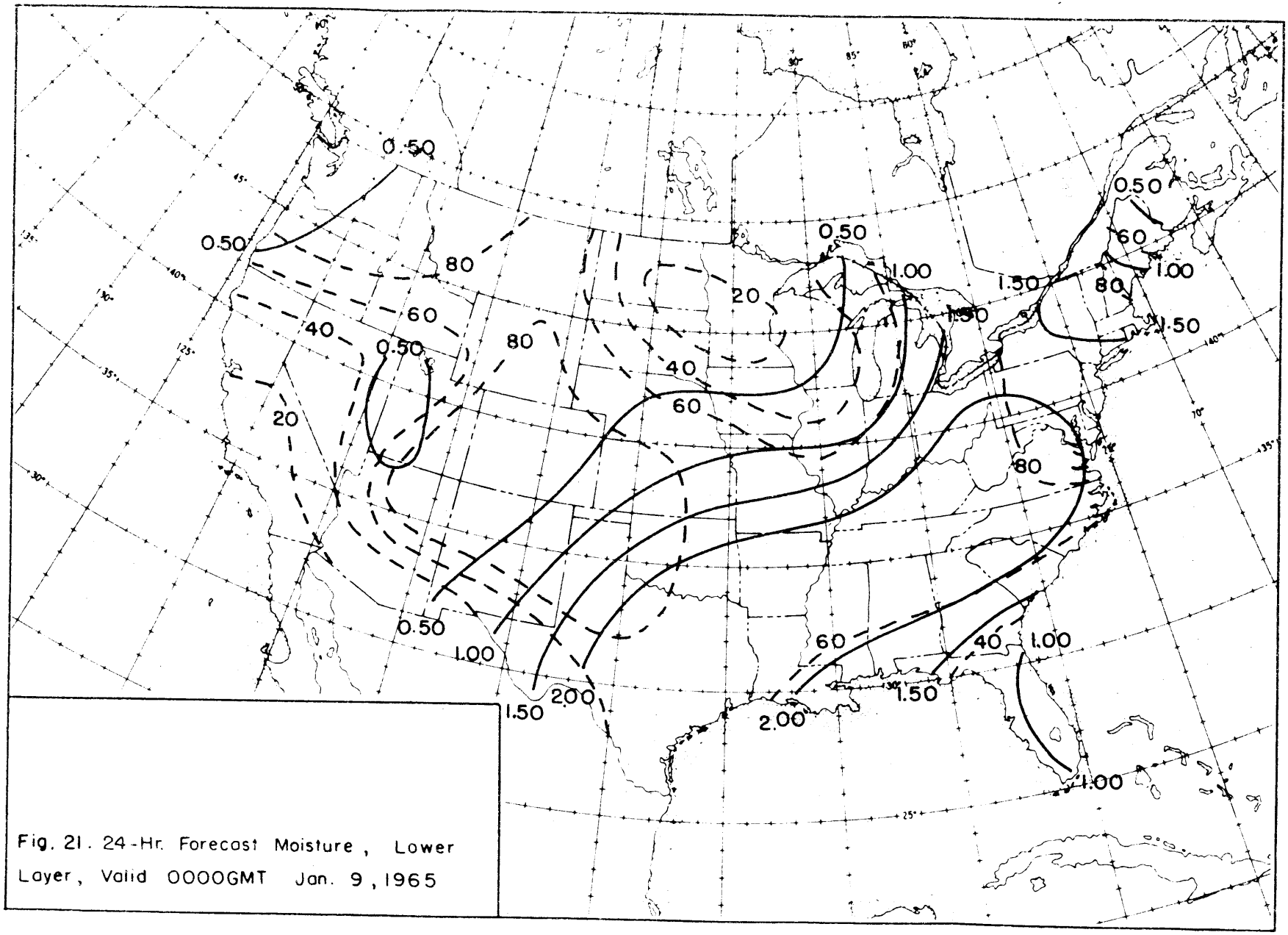

Fig. 21. 24-Hr. Forecast Moisture, Lower Layer, Valid 0000GMT Jan. 9, 1965

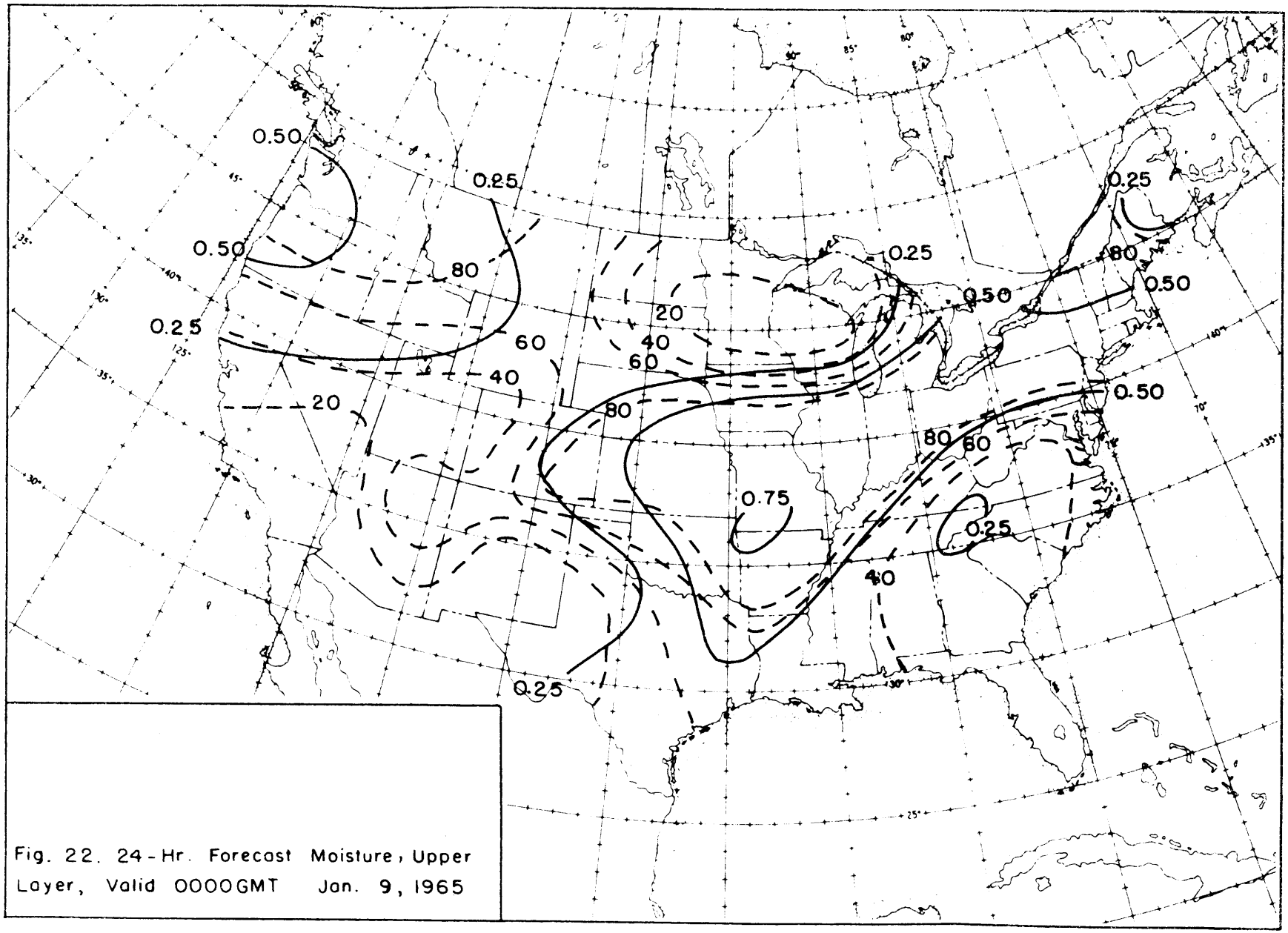

Fig. 22. 24-Hr. Forecast Moisture, Upper Layer, Valid 0000GMT Jan. 9, 1965

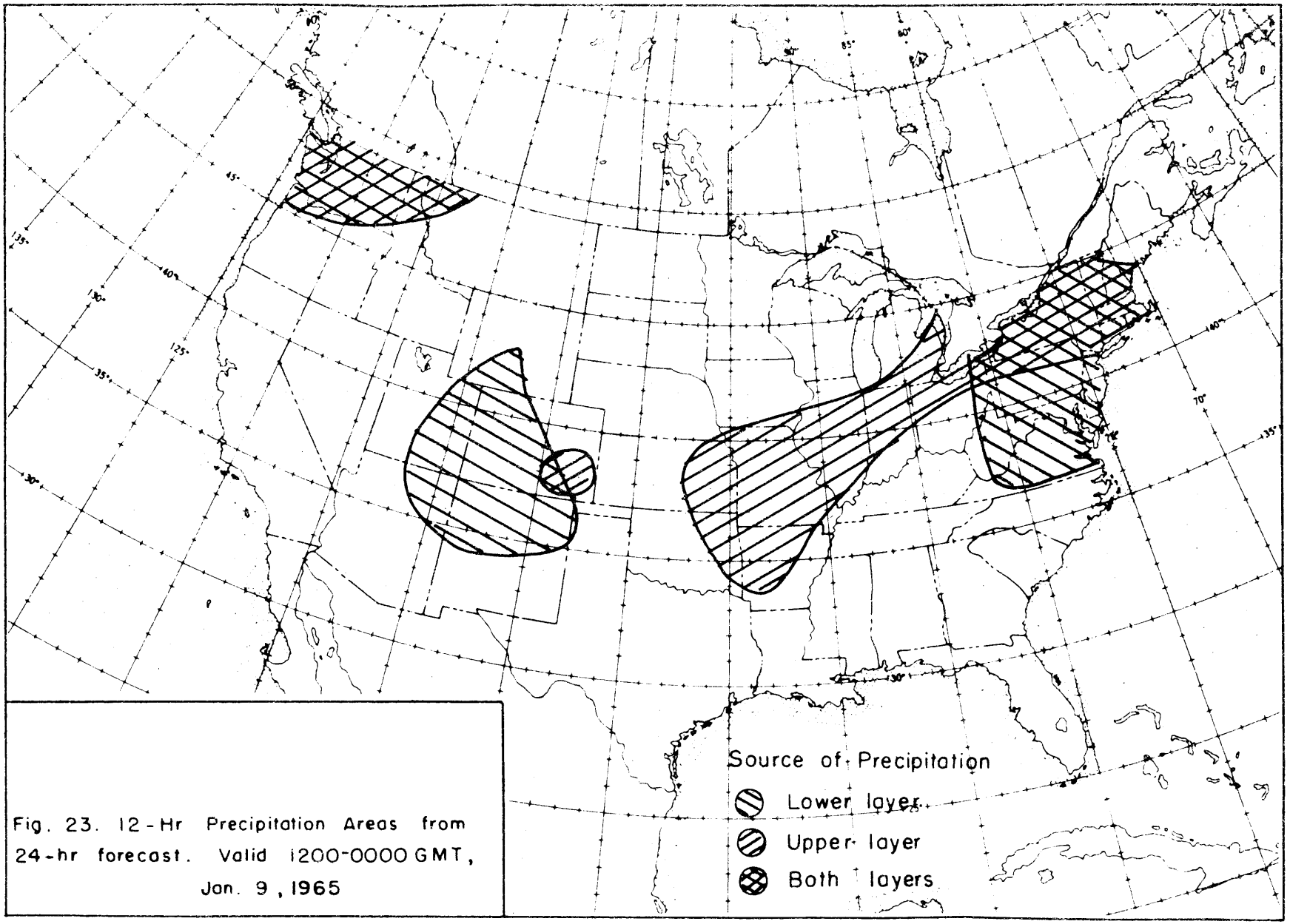

Fig. 23. 12-Hr Precipitation Areas from 24-hr forecast. Valid 1200-0000 GMT, Jan. 9, 1965

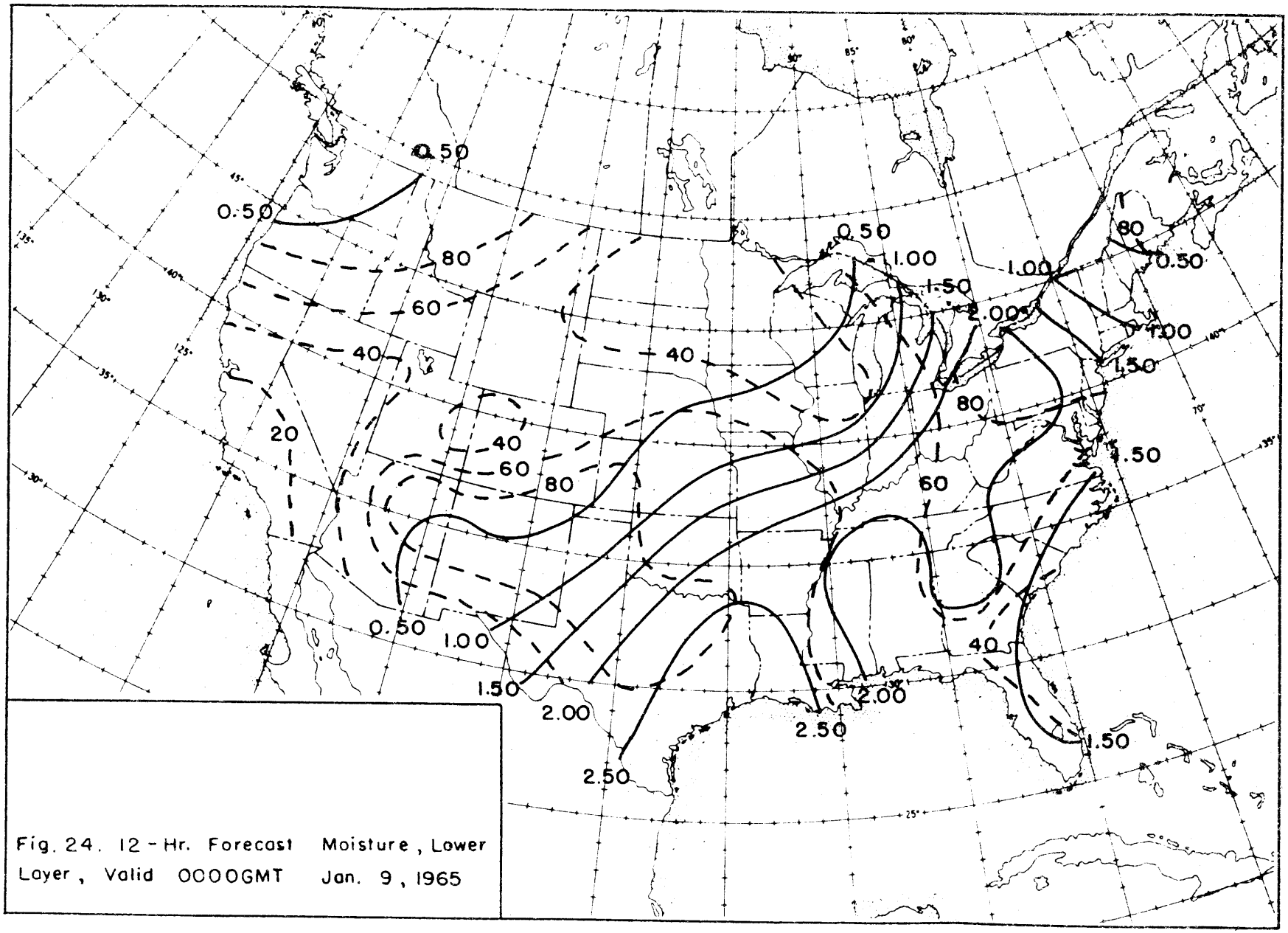

Fig. 24. 12-Hr. Forecast Moisture, Lower Layer, Valid 0000GMT Jan. 9, 1965

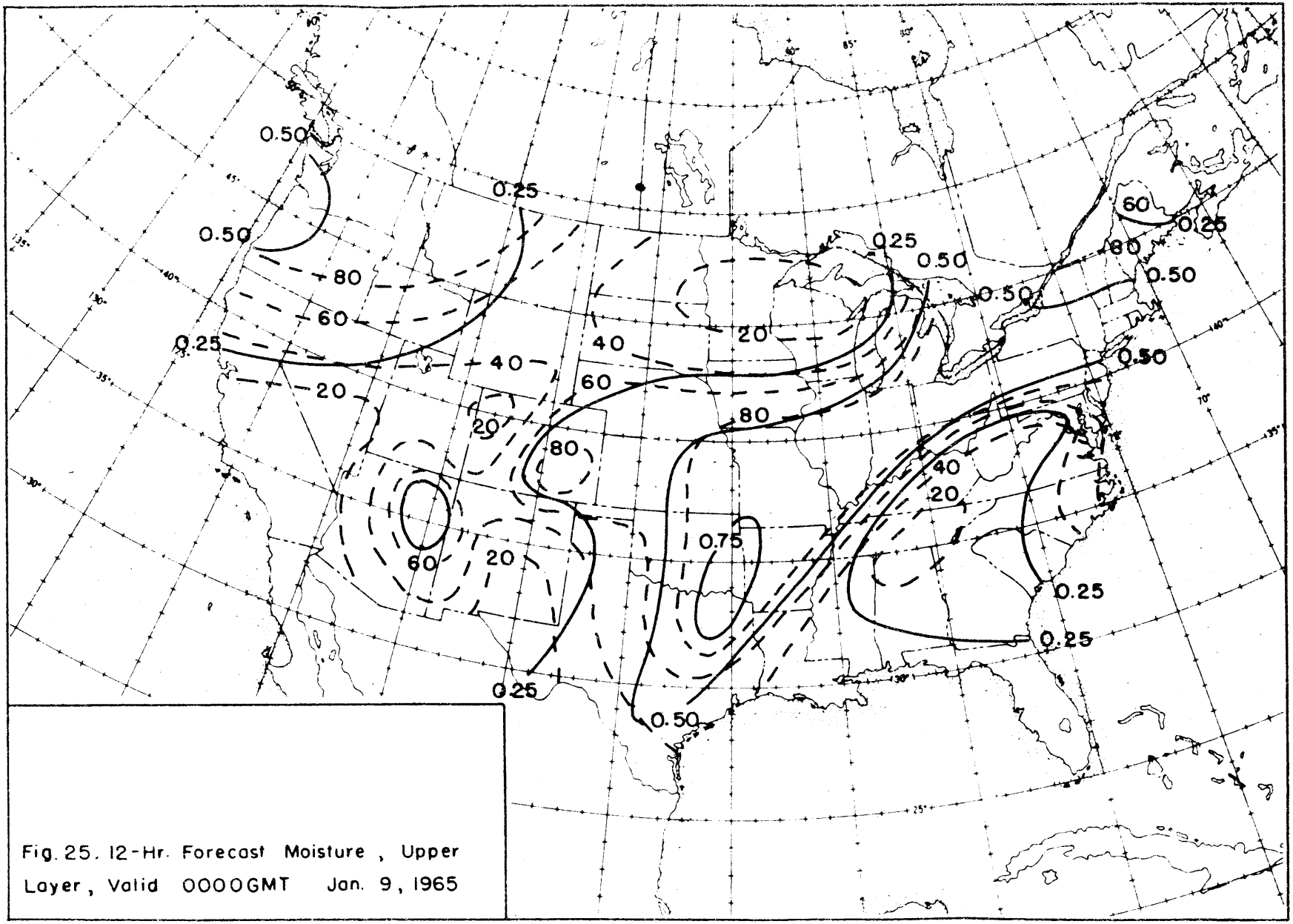

Fig. 25. 12-Hr. Forecast Moisture, Upper Layer, Valid 0000GMT Jan. 9, 1965

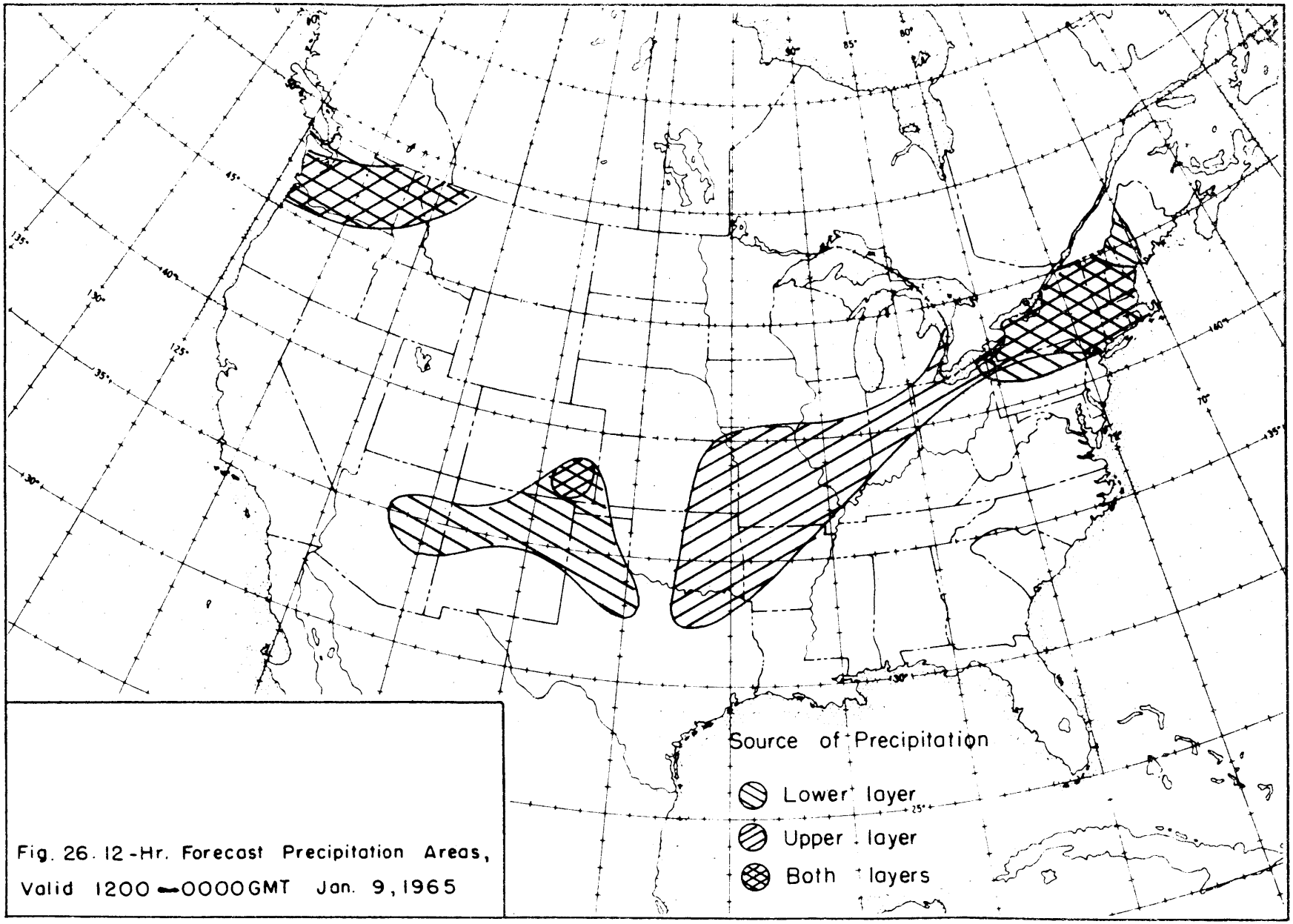

Fig. 26. 12-Hr. Forecast Precipitation Areas, Valid 1200 —0000GMT Jan. 9, 1965

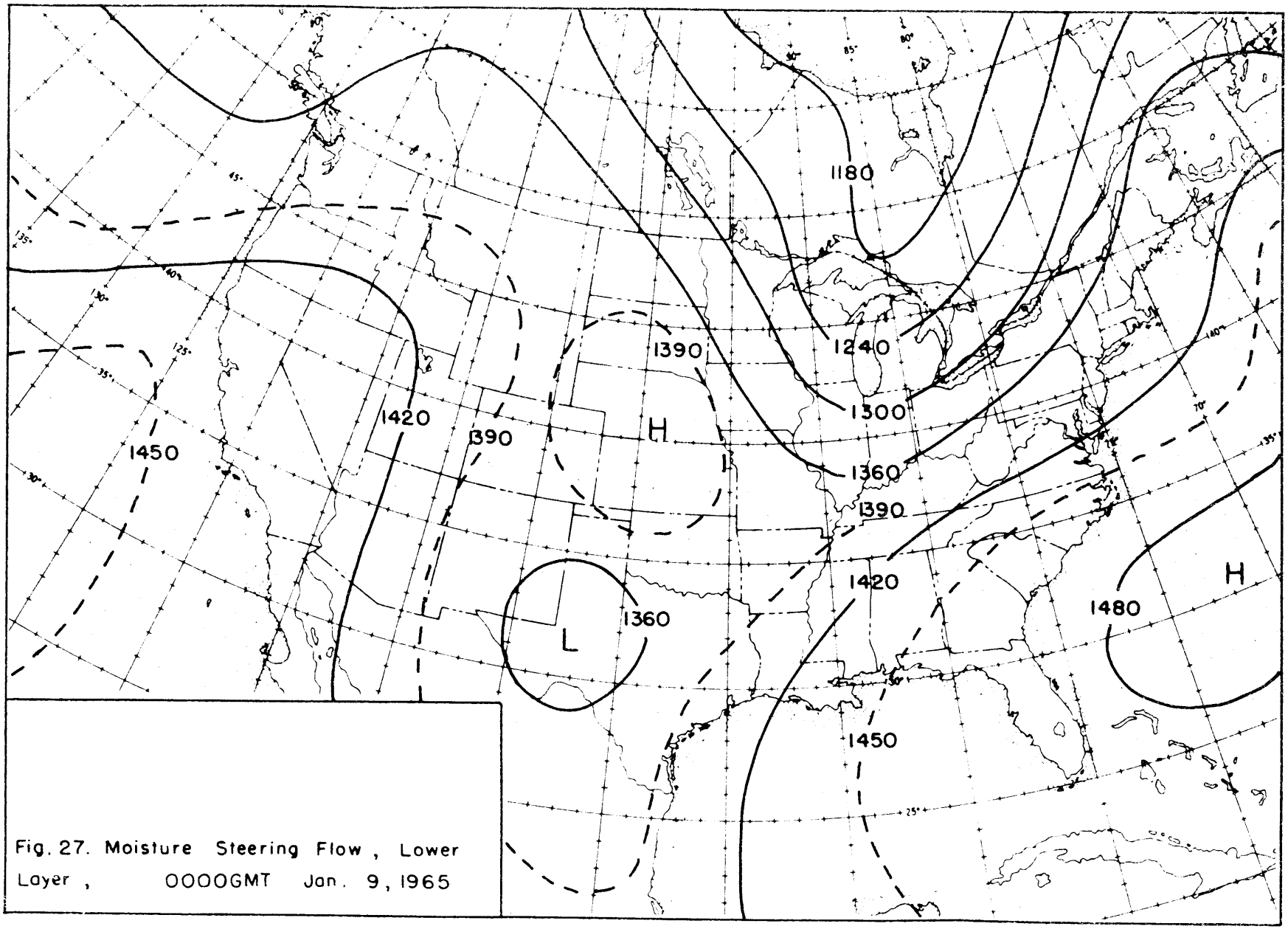

Fig. 27. Moisture Steering Flow, Lower Layer, 0000GMT Jan. 9, 1965

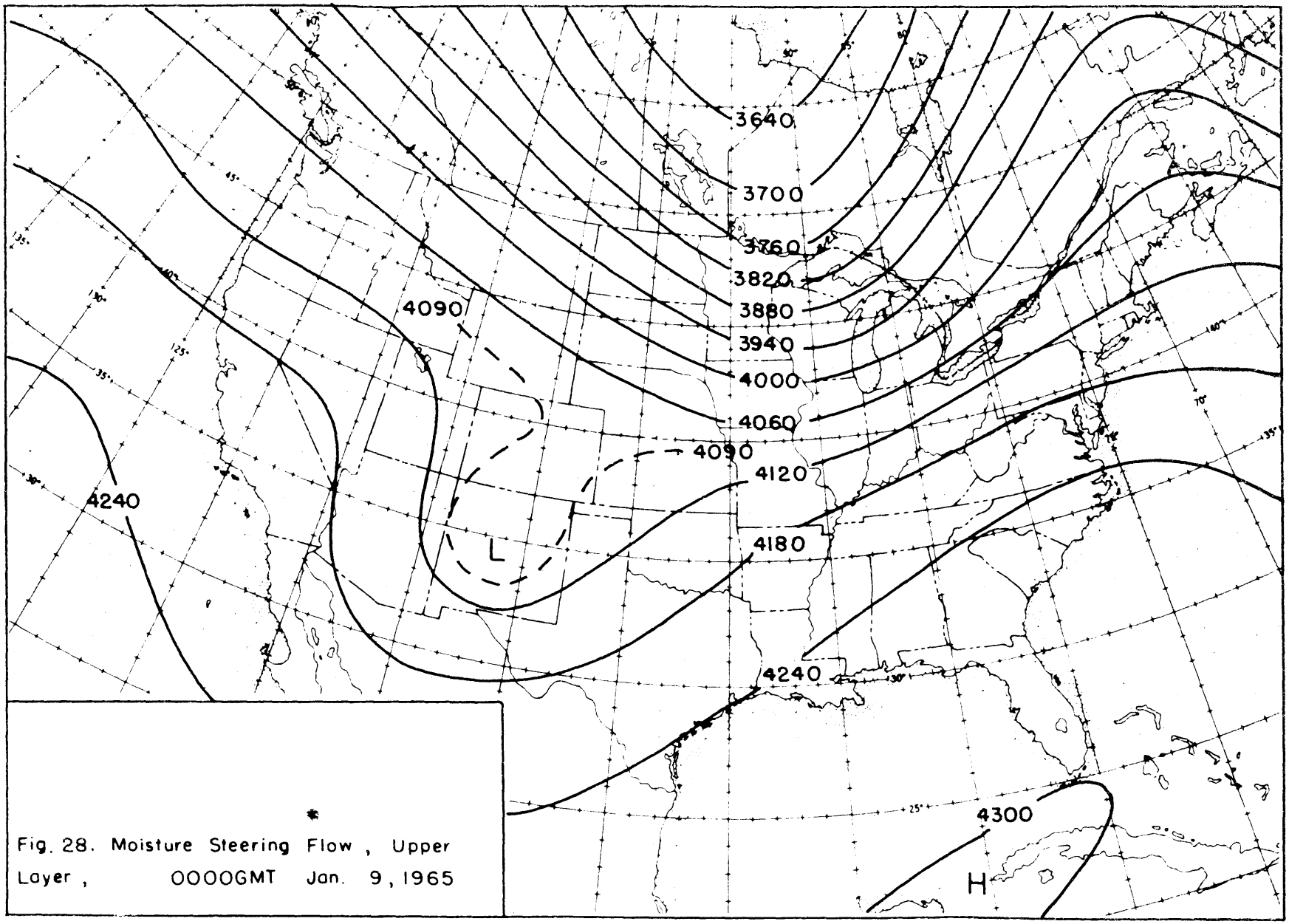

Fig. 28. Moisture Steering Flow, Upper Layer, 0000GMT Jan. 9, 1965

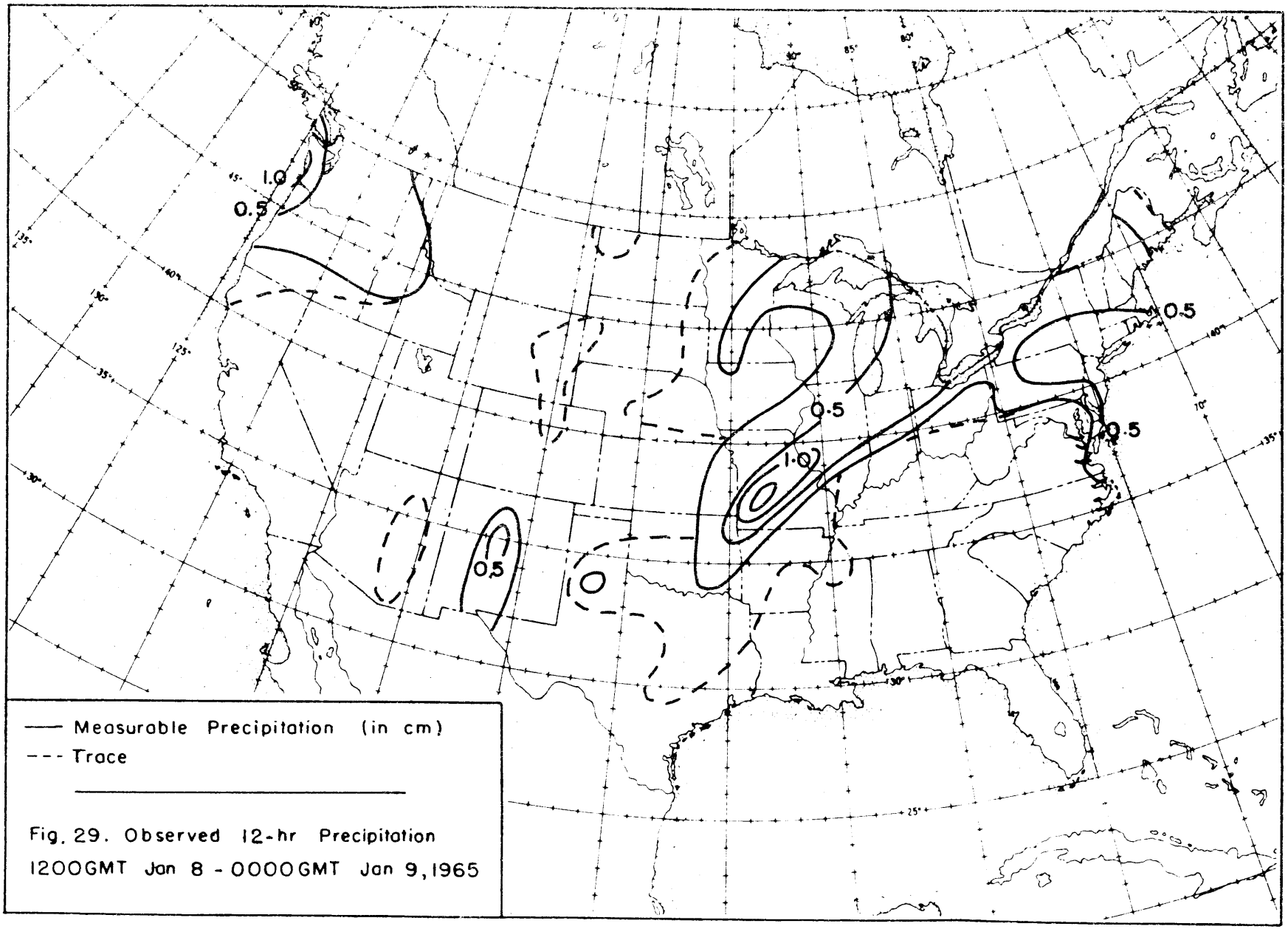

Fig. 29. Observed 12-hr Precipitation
1200GMT Jan 8 - 0000GMT Jan 9, 1965

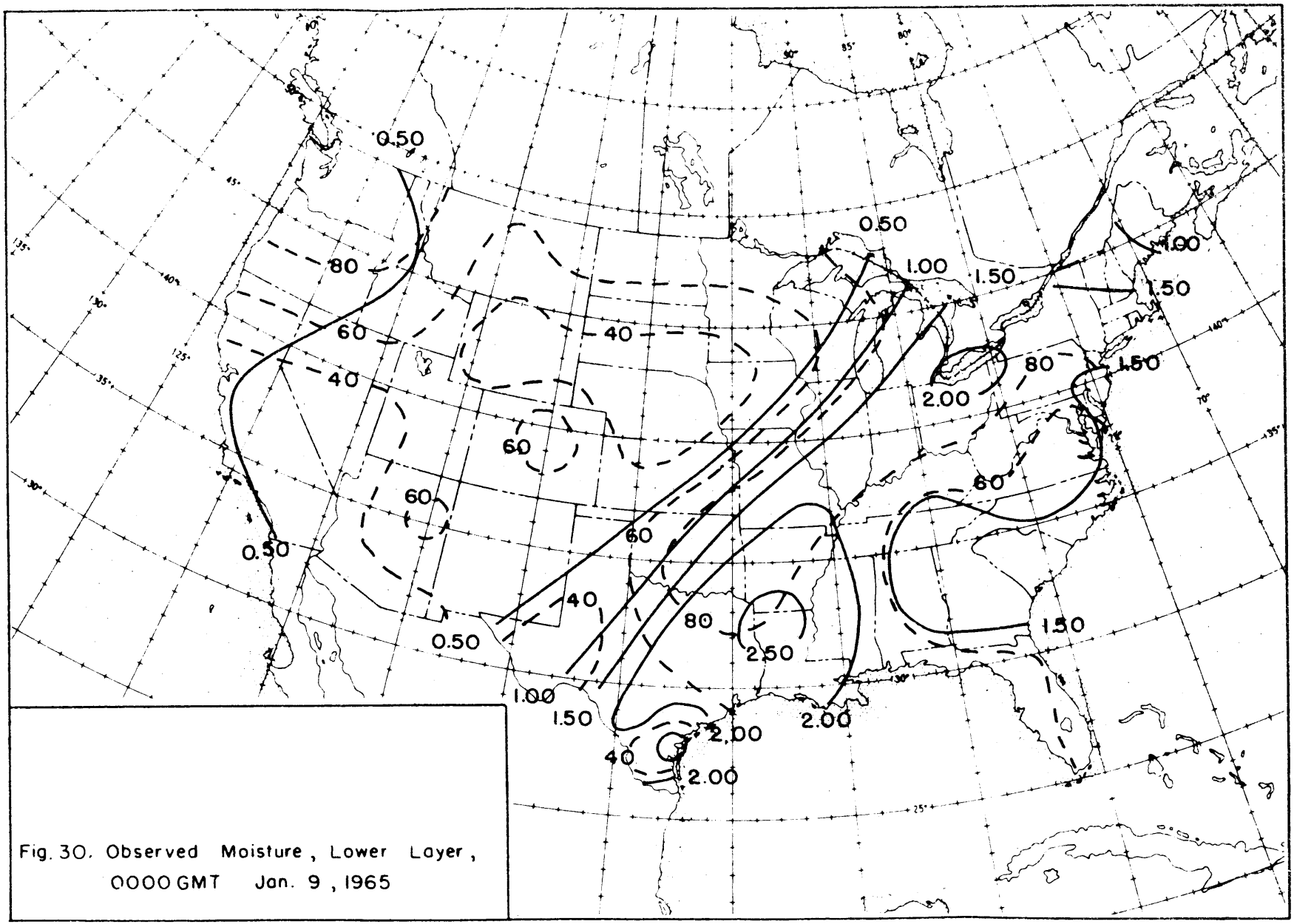

Fig. 30. Observed Moisture, Lower Layer, 0000 GMT Jan. 9, 1965

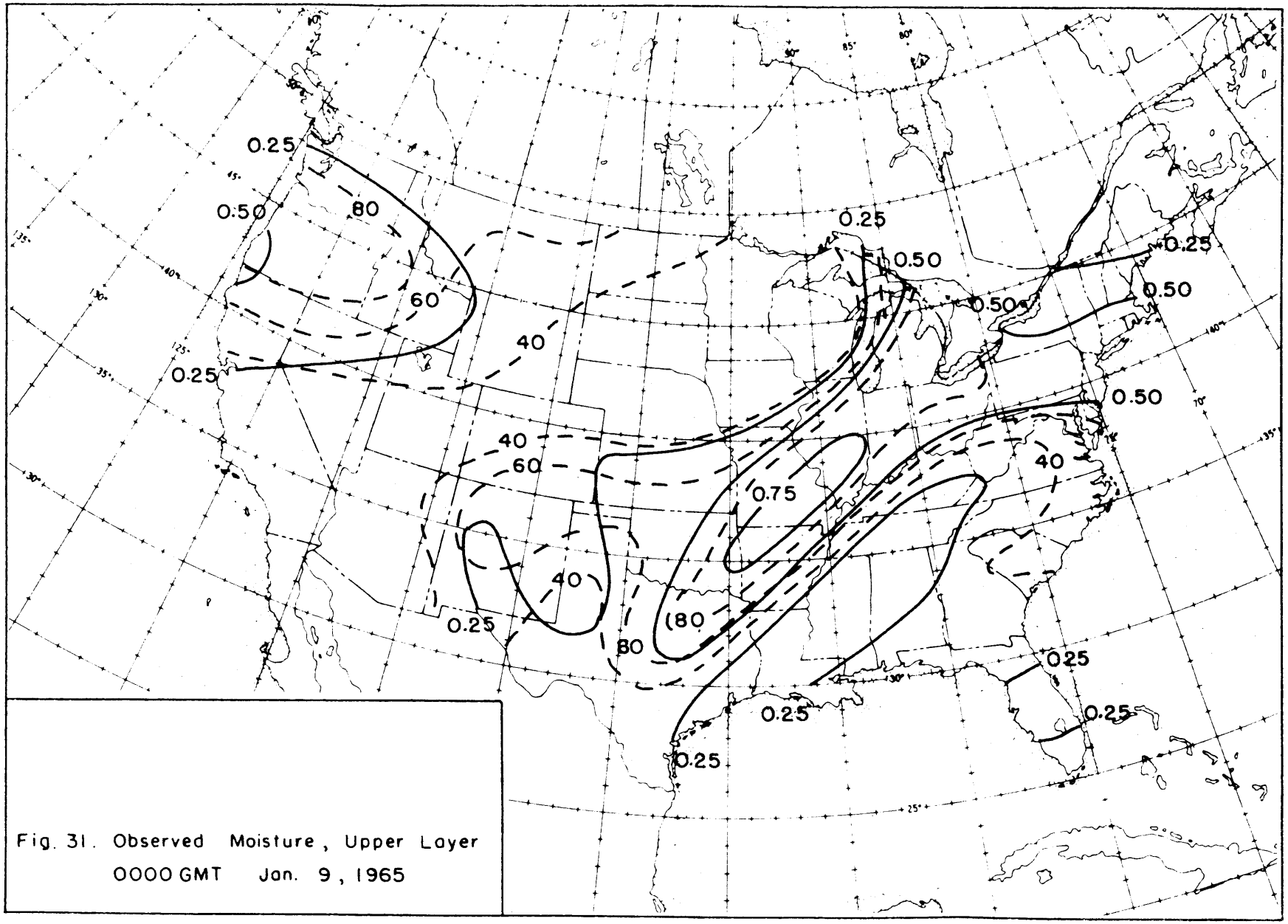

Fig. 31. Observed Moisture, Upper Layer
0000 GMT Jan. 9, 1965

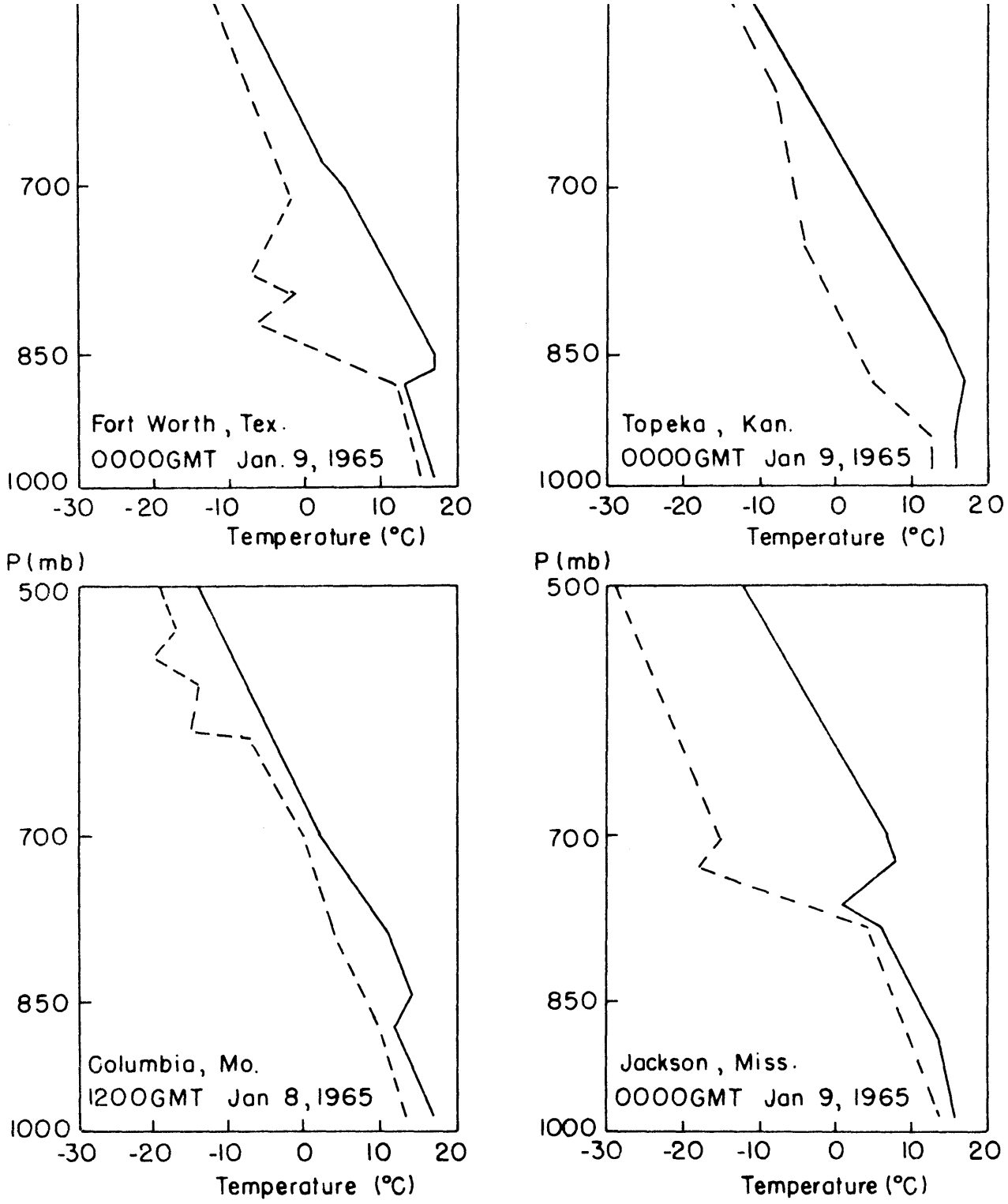
P(mb)
500
700
850
1000
-30 -20 -10 0 10 20
Temperature (°C)
Fort Worth, Tex.
0000GMT Jan. 9, 1965
Topeka, Kan.
0000GMT Jan 9, 1965
Columbia, Mo.
1200GMT Jan 8, 1965
Jackson, Miss.
0000GMT Jan 9, 1965

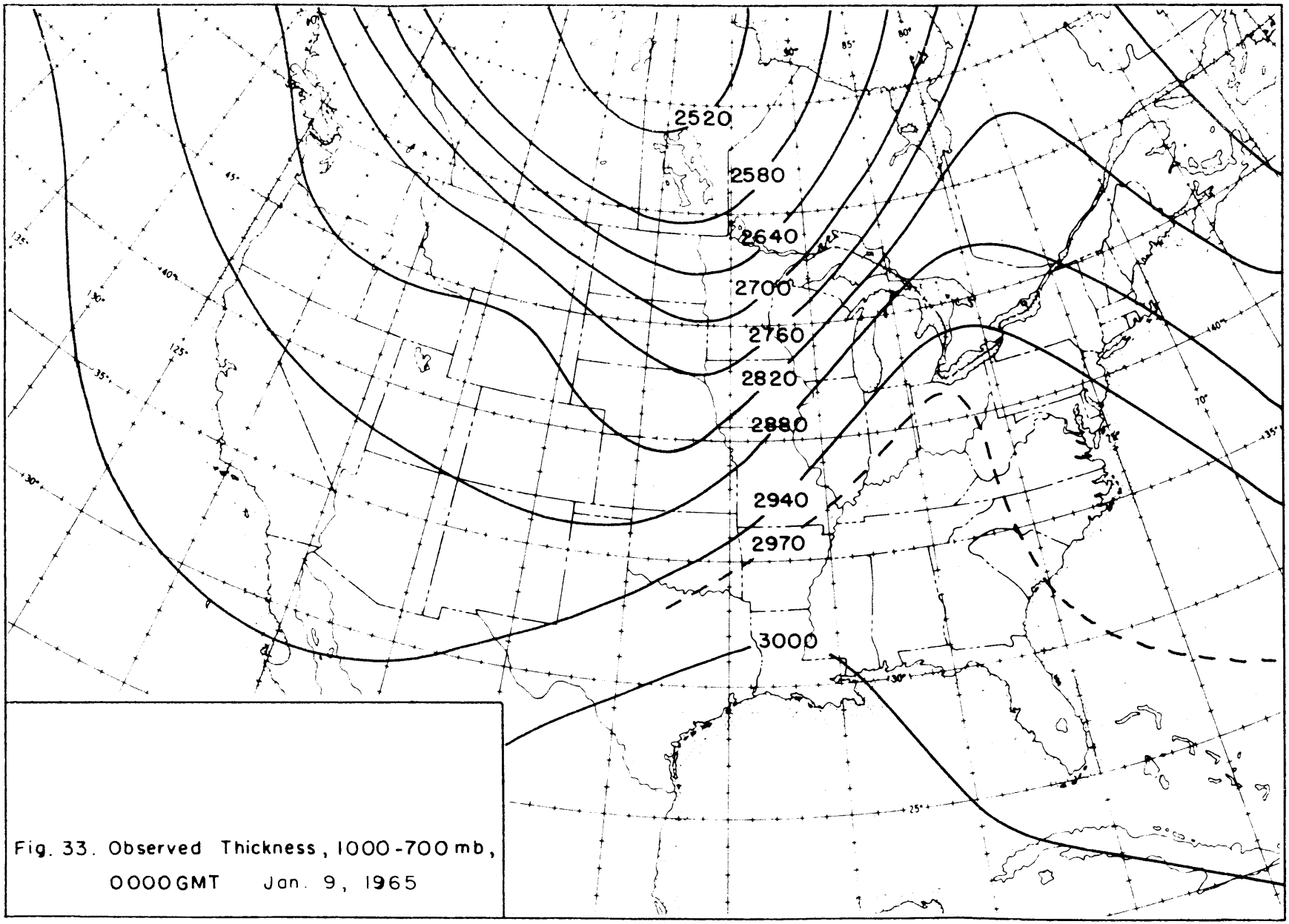

Fig. 33. Observed Thickness, 1000-700 mb, 0000 GMT Jan. 9, 1965

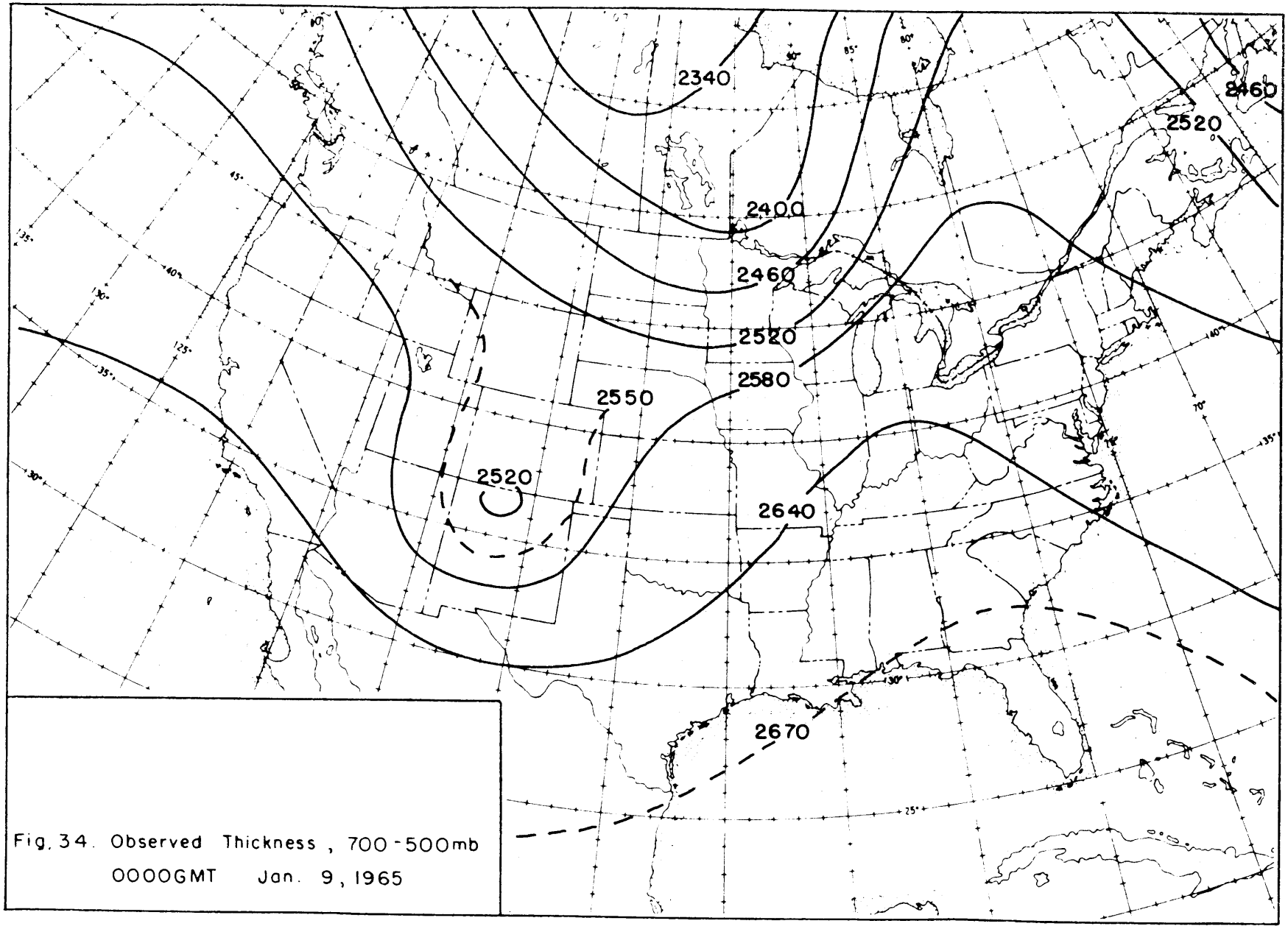

Fig. 34. Observed Thickness, 700-500mb
0000GMT Jan. 9, 1965